

# **ANALYSIS OF TRANSONIC TURBINE CASCADES INCLUDING REDESIGN OF BLADE PROFILES USING VELOCITY GRADIENT APPROACH**

A Thesis Submitted  
In Partial Fulfilment of the Requirements  
for the Degree of

**MASTER OF TECHNOLOGY**

by

**REKHLAL RANA**

to the

**DEPARTMENT OF AERONAUTICAL ENGINEERING**

**INDIAN INSTITUTE OF TECHNOLOGY, KANPUR**

**JULY, 1987**

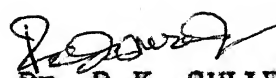
Dedicated to

My Reverend Parents

**CERTIFICATE**

This is to certify that the thesis entitled "Analysis of transonic turbine cascades including redesign of blade profiles using velocity gradient approach", submitted by REKHLAL RANA in partial fulfilment of the requirements for the degree of Master of Technology at Indian Institute of Technology, Kanpur is a record of bonafied research work carried out by him under my supervision and guidance. The work embodied in this thesis has not been submitted elsewhere for a degree.

Dated: July 16, 1987

  
Dr. R.K. SULLEREY  
ASSTT. PROFESSOR  
Dept. of Aeronautical Engineering  
Indian Institute of Technology,  
Kanpur

## ACKNOWLEDGEMENTS

I wish to record my deep sense of gratitude to Dr. R.K. Sullerey for suggesting the problem and supervising the study covered in this thesis. I am deeply indebted to him for his inspiring guidance, meticulous attention, constructive criticism and above all for his untiring devotion throughout the tenure of this work.

I would also like to thank my friends, Bharat Bhusan, G.K. Adil, A.K. Dikshit, Shachindra, Rajkumar, S.K. Shukla and D.K. Singh for their help at certain moments during this work.

I am also thankful to Mr. S.J. Gupta for his excellent typing of the manuscript. At the end, thank to all those who helped me directly or indirectly during this work.

  
REKHLAL RANA

CONTENTS	Page No.
Certificate	i
Acknowledgements	ii
Nomenclature	v
List of Figures	vii
Abstract	ix
CHAPTER I INTRODUCTION	1
1.1 Literature Survey	2
1.2 Incompressible Flow	2
1.3 Compressible Flow	4
1.4 Matrix Method	4
1.5 Finite Element Method	4
1.6 Time Marching Method	5
1.7 Streamline Curvature Method	6
1.8 Scope of present Investigation	8
CHAPTER II FORMULATION AND APPROACH TO SOLUTION	10
2.1 Formulation	10
2.2 Finite Difference Approximation	14
2.3 Calculation of Velocity and Density	18
2.4 Calculation of Critical Velocity	20
2.5 Calculation of maximum value of mass flow parameter	20
2.6 Calculation of leading edge and trailing edge radii	20
2.7 Calculation of surface length	20
2.8 Velocity Gradient Approach	20
2.9 Airfoil geometry	22
2.10 Determination of input for the design	23

CHAPTER III	COMPUTER PROGRAM	25
3.1	Introduction	25
3.2	Description of Input Data	26
3.3	Description of Normal Output	28
3.4	Overall program logic	29
CHAPTER IV	RESULTS AND DISCUSSION	33
4.1	CONCLUSIONS	37
4.2	SCOPE OF FUTURE WORK	37
	List of References	38
	Appendix A	41

## NOMENCLATURE

SYMBOL	DESCRIPTION
A	Coefficient in differential equation (2.4)
B	Coefficient in differential equation (2.4)
$B_x$	Axial chord, meters
b	Stream channel thickness normal to meridional streamlines, meters
$C_{pi}$	Pressure coefficient
H	Camber distance parameters, meters
m	Meridional streamline distance, meters
P	Pressure
R	Gas constant, J/(kg)(k)
$R_1, R_2$	Radii of leading and trailing edge circles, meters
r	Radius from axis of rotation to meridional streamchannel mean line, meters
s	Angular blade spacing or pitch, radian
T	Temperature, k
t	Time, second
u	Stream function
V	Absolute fluid velocity, meters/second
W	Fluid velocity relative to blade, meters/second
w	Mass flow per blade flowing through stream channel, kg/sec
z	Axial co-ordinate, meters
$\alpha$	Angle between meridional streamline and axis of rotation, radian
$\beta$	Angle between relative velocity vector and meridional plane, radian

$\beta_1$	Inlet gas flow angle, degree
$\beta_2$	Outlet gas flow angle, degree
$\beta_\lambda$	Gaging angle, degree
$\beta^*_1, \beta^*_2$	Metal angles at leading and trailing edges, degrees
$\Delta\beta^*_1, \Delta\beta^*_2$	Wedge angles at leading and trailing edges, degrees
$\gamma$	Specific heat ratio
$\rho$	Density, $\text{kg/m}^3$
$\theta$	Relative angular co-ordinate, radian
$\lambda$	Pre-rotation, $(rV_\theta)$ , $\text{meters}^2/\text{second}$
$\omega$	Rotational speed, radian/second
$\tau$	Throat length, radian
$\Gamma$	Uncovered turning, degrees
$\eta$	Outer normal to region
$\Omega$	Over-relaxation factor

## SUBSCRIPTS

Cr	Critical velocity
in	Inlet or upstream
j	dummy variable
Le	leading edge
m	Component in direction of meridional streamline
out	Outlet or downstream
r	radial component
te	trailing edge
z	axial component
$\theta$	tangential component
'	absolute stagnation condition
"	relative stagnation condition

## LIST OF FIGURES

No.	TITLE	Page No.
1.1	Schematic view of blade to blade, Plane $S_1$ , and meridional plane $S_2$ .	45
2.1	Cylindrical co-ordinate system and velocity components.	46
2.2	Blade to blade surface of revolution showing $m-\theta$ co-ordinates	47
2.3	Flow in a mixed-flow stream channel	48
2.4	Finite flow region of turbine cascade	49
2.5	Notation for adjacent mesh points and mesh spaces	50
2.6	Mesh points on lower boundary	51
2.7	Mesh points on upper boundary	52
2.8	Co-ordinate system and cascade geometric parameters	53
3.1	Geometric input variables on blade to blade stream surface	54
3.2	Geometric input variables describing stream channel in meridional plane	55
3.3	Finite difference mesh in blade to blade solution region.	56
3.4	Flow chart for subroutine calling sequence	58
4.1A	Comparison of blade surface velocities with experimental data for stator case.	58
4.1B	Comparison of blade profile for stator guide vane	59
4.2	Comparison of blade surface velocities for stator guide vane	60

4.3	Comparison of surface pressure coefficient distribution for stator guide vane	61
4.4	Comparison of blade profile for stator guide vane	62
4.5	Comparison of blade surface velocity for stator guide vane	63
4.6	Comparison of surface pressure coefficient distribution for stator guide vane	64
4.7	Comparison of blade profile for turbine rotor case.	65
4.8	Comparison of blade surface velocities for rotor case	66
4.9	Comparison of surface pressure coefficient distribution for turbine rotor case.	67

## ABSTRACT

The present investigations comprises of an implementation of a computer code using streamline curvature method for the flow over blade to blade plane of turbine cascades and subsequent application of this code for redesign of blade profiles. The program is essentially for subsonic flow except for some local regions of supersonic flow. The transonic flow solution is obtained by a combination of a finite difference, stream function solution and a velocity gradient solution. For the solution of second degree equation of stream function the finite difference technique is used at the reduced weight flow. Subsequently the velocity gradient approach makes use of the results of this analysis for full weight flow calculations. The program input includes cascade geometry, inlet and outlet flow angles and stagnation flow conditions and provide the blade surface velocities and streamline co-ordinate in passage output. The computed blade surface velocities have been compared with the available experimental data. A systematic computational design system for turbine cascade is incorporated to redesign and optimise the airfoil geometry to improve the blade surface velocity distribution. The modified profiles thus obtained show improvement over the original ones and are likely to have lower profile losses due to reduced suction surface diffusion.

## CHAPTER 1

### INTRODUCTION

In order to predict the performance of a turbomachine, an analysis of flow through it, is required. The internal flow through turbomachines is usually three dimensional viscous and unsteady. The extreme complexity of the flow makes it difficult to determine the velocity distribution and flow directions throughout the flow field, simultaneously taking into account all the factors. The turbine design problem therefore is usually divided into three major steps, the first is the determination of the requirement of the flow, work and speed. The second step is the evolution of the velocity diagrams which should be consistent with the desired efficiency and number of stages. The third step is the design of the blading that will provide the necessary flow angles and velocities required by the velocity diagrams.

The essence of the classical approach is the splitting up of the three dimensional problem into two separate two dimensional problems. The first problem is that of the flow in the meridional plane having  $r$ - $z$  coordinates. The plane extends from hub to tip. The second plane is the cascade plane also known as blade to blade plane having the  $z$ - $\theta$  coordinates. The Fig. 1.1 shows the blade to blade and meridional planes as S1 and S2 surfaces respectively.

Through flow equations have been developed for these planes. Advent of modern computers with their vast memory storage capabilities enables one to solve the extremely complicated three dimensional non viscous equations. The computations using the computers forms a framework for both rapid preliminary evaluations as well as for more detailed final designs.

A successful design scheme for turbomachinery cascades would provide a calculation tool by which cascade geometry could be computed from certain design inputs and provide a subsequent procedure by which optimum geometries may be determined and chosen. The design procedure usually starts from known flow conditions ahead of and behind the leading and trailing edges respectively. The thermodynamic states and flow velocities at the inlet and outlet of the cascade having been calculated in advance. The design problem of a cascade is therefore to find out the blade profiles that lie on a surface of revolution and also satisfy imposed design requirements.

### 1.1 LITERATURE SURVEY

### 1.2 INCOMPRESSIBLE FLOW

For incompressible flows, the problem is posed mathematically as the solution of the Laplace equation

$$\frac{\partial^2 \phi}{\partial x^2} + \frac{\partial^2 \phi}{\partial y^2} = 0 \quad \text{in a potential field for specified boundary}$$

conditions. Direct problem approach for incompressible potential

flow needed few specific informations such as cascade geometry, inlet flow angles and discharge conditions. There were various methods available for the solution of the incompressible potential flows namely conformal transformation, singularity method etc. The conformal transformation method provides solution for isolated airfoil of arbitrary shape. It applied Kutta-Joukowski transformation for the solution near the pointed trailing edge and an integral equation was solved iteratively. This method finds notable applications for cascades. The singularity method had been developed for thin airfoils with small camber and pointed trailing edge. Theodorsen transformation has been used to determine the pressure coefficient around the airfoil. The resulting pressure distribution is corrected for interference effects due to other airfoils in the cascade, using suitable distribution of vortices and sources in the singularity method.

The pioneer of cascade theory was Chaplygin (1). A rapid approximation theory was given by Erwin and Yacobi (2) based upon known flow around an isolated aerofoil. Wu and Brown (3) gave a simple solution which is best suited to closely-spaced turbine blading. Theodorsen (4) had produced a solution to the direct problem for isolated aerofoils of arbitrary shape.

### 1.3 COMPRESSIBLE FLOW

The inlet Mach Number for turbine blade rows usually has a high subsonic value and therefore a theoretical approach of subsonic compressible flow through cascades is essential. Extensive work has been done for the case of compressible flows and various compressible flow theories have been developed. Matrix method, Finite element method, Time marching method and Streamline curvature method have been used with success.

### 1.4 MATRIX METHOD

In the matrix through flow method the grid is formed and the nonlinear stream function is expressed in the form of quasi linear equations. The contribution made by Marsh (5) was in his selection of a very appropriate irregular finite difference grid. The finite difference equation is then formed and solved for stream function at all mesh points. The new stream function distribution is then used to form a new set of equations and the process is repeated until a convergence criterion is satisfied. As with the iterative procedures it is good practice to increase the inlet Mach Number in gradual steps to the desired value.

### 1.5 FINITE ELEMENT METHOD

Finite element method is more general and has advantage of flexibility as compared to finite difference methods. It allows the use of an irregular grid and higher order elements may be imposed locally to improve accuracy where boundaries are irregular.

Finite element may be chosen such that grid points coincide with the boundary, since the computation locations are also the corners of the elements. The finite element method proceeds by the formation of integrals of approximation over the domain under consideration. This is more readily achieved by identification of a variational principle requiring maximization of a scalar function over the domain.

One technique which seems to work for subsonic and low transonic flows is the local linearisation approach of Habashi (6). He linearise the equations with regard to the local Mach Numbers throughout the region. A separate linearisation is therefore performed for each element, the variational principle for that element being based on the Laplace equation for the locally linearised compressible flows. This linearisation is deployed within an iterative scheme and provides stability and rapid convergence for all subsonic Mach Numbers. Adler and Krimmerman (7) adopt a different approach by rewriting the governing equations in the form of Poisson equations having right hand side composed of known functions.

## 1.6 TIME MARCHING METHOD

The recent development in cascade flows in blade to blade plane includes time marching technique for the throughflow calculations. For the case when there is locally supersonic flow, the region is no longer elliptic but is hyperbolic. The problem of mixed, elliptic and hyperbolic domains with strong discontinuities

has been solved by use of 'time-marching' techniques using the governing time dependent equations for compressible flow. This method demonstrated the ability to capture strong shocks. McDonald(8) assume isentropic flow in his finite volume time marching approach. Good agreement is obtained between isentropic time marching method and experimental data for cases having local Mach Number as high as 1.43. In an improved scheme Denton (9) choose to solve the energy equations thus considering entropy variables in the flow field. Novick (10) produced a predictor corrector time marching solution to the Navier Stokes equation and demonstrated good agreement with experimental results for a transonic flows.

#### 1.7 STREAMLINE CURVATURE METHOD

The method is so named because the equations of motion are used in a form which relates the cross stream velocity gradient to the radius of curvature of the streamline. Since the radius of curvature of a streamline is a geometrical factor and stream spacing is determined by the continuity equation, it is relatively simple method to solve the equations of motion for any given geometry. The advantage of these methods appear to be efficiency of operation and the capability to consider velocities above the critical. The methods have originated using streamline and 'quasi orthogonals' which are simply lines passing from one channel wall to the other, in an arbitrary direction. It is advantageous to switch to full orthogonal grid for transonic cascades.

In a typical streamline curvature, programme the input data are differentiated twice and the values obtained are used in the velocity gradient equation. A start is made with approximate velocities along the mid streamline obtained from the previous iteration. A numerical integration is then performed in both directions to find the blade surface velocities. The velocity levels are then adjusted to satisfy continuity by iterative technique. In order to ensure rapid convergence an approximate damping factor must be chosen. The change in velocity gradient appears to be sensitive to the convergence criterion and this is reduced between iterations to prevent divergence.

The streamline curvature technique is solved by two distinct techniques one using normals to the flow by Jansen (11) and Binden and Carmichael (12) and the other using quasi-orthogonals by Theodore Katsanis (13) and Wilkinson (14). The approach using normals to the flow has been used for two dimensional cases and has been less good than quasi-orthogonals in many respects. Quasi orthogonals are in practice near straight lines and proceed from one wall to the other of the channel or one blade surface to other, confining the flow. All the mass flow crosses the quasi-orthogonals and is used to satisfy the continuity equation, by adjusting the velocity along the quasi-orthogonals to obtained correct mass flow. The velocity gradient relationship along the quasi orthogonals is derived from momentum energy and entropy equations. Since all the terms of right hand side are not known iterative techniques are used to solve the simultaneous equations. This approach is

basically applicable to subsonic flows but can also deal with transonic flows.

Considerable work has been done on non-series airfoil design over series airfoil for highly loaded turbine blade profiles by Monello and Mitchell (24). In their work the non-series airfoils were designed from series airfoils and they exhibit considerable improvement over the series airfoils. Z.Q. Ye (23) describes a computational design system for two dimension turbine cascade. He has made a sequence of calculations in which airfoil profiles are designed from velocity diagram requirements and specified geometric parameters.

#### 1.8 SCOPE OF PRESENT INVESTIGATIONS

The present work included systematic computational design system for two dimensional turbine cascades using streamline curvature scheme for transonic flow. Considerable efforts have been made to implement the program given in Ref. 21. As the program in Ref. 21 has been developed after a series of modifications over the previous program given in Ref. 17,18,19 and 20, as such all the subroutines are not explained in a single source. Therefore to fully understand and implement the program required considerable time and effort. The program has been run and tested for several cases. The computational results are compared with experimental results. There is good agreement between the results so obtained.

The work also includes a sequence of calculations to modify to existing blade profiles using the technique given by Ye to yield better blade surface velocity distribution. Thus in turn is reported to reduce the profile losses over the blade surfaces and to curb the tendency of early separation. For such investigations three different types of stator and rotor blades were chosen and for each case velocity distribution and pressure coefficient distribution over surfaces are calculated. The results have been compared with the results of the original profile. In all these cases the blades were highly loaded and the loading coefficient ranged from 0.8 to 0.94. The outlet MACH NUMBER for rotor and stator blade profile ranged from 0.58 to 1.05.

## CHAPTER 2

## FORMULATION AND APPROACH TO SOLUTION

## 2.1 FORMULATION

The solution for the transonic flow is to be obtained in two stages. In the first stage the calculations are done for reduced weight flow by finite difference solution for stream function. The weight flow is reduced sufficiently so that the flow becomes subsonic throughout the passage.

In the second stage the calculations are done with full weight flow using velocity gradient (streamline curvature) method. The solution obtained by reduced weight flow is used as input for full weight flow in velocity gradient solution.

The basic reason behind the splitting of the solution in two stages is the limitations of the respective methods. The finite difference solution of the stream function equation is limited to strictly subsonic flows. On the other hand a simple velocity gradient method is limited to a well guided channel. The purpose herein is to combine these methods so as to extend the range of cases.

The following simplifying assumptions are used in deriving the equations for both stages.

1. The fluid is perfect gas
2. The flow is steady relative to the blade
3. The flow is irrotational

4. The fluid is non-viscous and there is no heat transfer
5. The blade to blade surface is a surface of revolution
6. There should not be any velocity component normal to the blade to blade surface.
7. The stagnation temperature is uniform across the inlet
8. The magnitude and direction of velocity across upstream and downstream boundaries are to be uniform.
9. The only forces are those due to momentum and pressure gradient
10. The relative velocity is subsonic for the first stage calculations only. It may be either subsonic or supersonic for the second stage calculations.

The coordinate system is shown in Fig. 2.1. The variables  $r$  and  $z$  are not totally independent on a stream surface and one of these variables can be eliminated. Therefore it is better to use meridional coordinate ' $m$ ' as independent variable in place of  $r$  and  $z$ . Thus ' $m$ ' and ' $\theta$ ' become the two basic independent variable. Blade to blade surface of revolution is shown in Fig. 2.2 and flow in mixed flow stream channel is shown in Fig. 2.3.

For the mathematical formulation of the problem the stream function is used. The basic differential equation which must be satisfied by the stream function under the given assumptions is

$$\frac{1}{r^2} \frac{\partial^2 u}{\partial \theta^2} + \frac{\partial^2 u}{\partial m^2} - \frac{1}{r^2} \frac{1}{\rho} \frac{\partial \rho}{\partial \theta} \frac{\partial u}{\partial \theta} + \left( \frac{\sin \alpha}{r} - \frac{1}{b \rho} \frac{\partial (b \rho)}{\partial m} \right) \frac{\partial u}{\partial m} = \frac{2 b \rho \omega}{w} \sin \alpha \quad (2.1)$$

The description and derivation of the above equation is given in Ref. 15.

The streamfunction  $u$  is to be normalised so that it has the value '0' on the upper surface of the lower blade and '1' on the lower surface of upper blade. The derivatives of the streamfunction satisfy

$$\frac{\partial u}{\partial m} = - \frac{b \rho}{w} w_{\theta} \quad (2.2)$$

$$\frac{\partial u}{\partial \theta} = \frac{b \rho r}{w} w_m \quad (2.3)$$

The boundary conditions used for the region ABCDEFGH for finite flow region is shown in Fig. 2.4 are as follows.

Boundary segment	Boundary conditions
AB	- $u$ is 1 less than the value of $u$ on GH at the same $m$ co-ordinate
BC	- $u = 0$
CD	- $u$ is 1 less than the value of $u$ on EF at the same $m$ co-ordinate
DE	- $\left(\frac{\partial u}{\partial \eta}\right)_{out} = - \frac{\tan \beta_{out}}{s r_{out}}$
EF	- $u$ is '1' greater than the value of $u$ on CD at the same $m$ co-ordinate
FG	- $u = 1$
GH	- $u$ is '1' greater than the value of $u$ on AB at the same ' $m$ ' co-ordinate
AH	- $\left(\frac{\partial u}{\partial \eta}\right)_{in} = - \frac{\tan \beta_{in}}{s r_{in}}$

The equation (2.1) is no longer elliptical for locally supersonic flows but it becomes hyperbolic. In such regions velocity gradient approach has been used for calculations. Simplified velocity gradient equation is given below

$$\frac{\partial W}{\partial \theta} = AW + B \quad (2.4)$$

where

$$A = r^2 \cos^2 \beta \frac{\partial^2 \theta}{\partial m^2} + \sin \alpha \tan \beta (1 + \cos^2 \beta) \quad (2.5)$$

is used on blade surface

$$A = \sin^2 \left( \frac{2 \frac{\partial^2 u}{\partial \theta \partial m}}{\frac{\partial u}{\partial m}} - \frac{\frac{\partial u}{\partial \theta}}{\left( \frac{\partial u}{\partial m} \right)^2} \frac{\partial^2 u}{\partial m^2} - \frac{\frac{\partial^2 u}{\partial \theta^2}}{\frac{\partial u}{\partial \theta}} \right) + \sin \alpha \tan \beta (1 + \cos^2 \beta) \quad (2.6)$$

is used at interior points and

$$B = r \tan \beta \frac{\partial W}{\partial m} + \frac{2 r \sin \alpha}{\cos \beta} \quad (2.7)$$

The description and derivational of the above equations is given in Appendix 'A'. The quantities used in above equations are known if solution of equation (2.1) is known. Therefore, by using finite difference technique an approximate solutions for reduced weight flow is obtained, such that the streamlines for the two flows are nearly close. For the incompressible flow there should not be any change in streamlines if  $\omega$  is reduced in the same proportion as  $w$ . This can be seen in equation (2.1), since coefficient

are constant for incompressible flow and equation (2.1) does not change if  $\frac{\omega}{w}$  is kept constant. There will be change in streamline shapes for compressible flow case and factor  $\frac{\partial W}{\partial m}$  which is proportional to weight flow for incompressible case is not same strictly. However, for many cases the error introduced by using quantities in equation (2.5) , (2.6) and (2.7) from reduced weight flow solution is not significant.

The equation (2.4) can be solved numerically along ' $\theta$ ' co-ordinate (i.e. at constant  $m$ ), by using approximate value of  $A$  and  $B$  calculated by finite difference technique for completely subsonic flow. The continuity equation for flow through cascade is

$$\int_{\theta_1}^{\theta_2} \rho W \cos \beta \, b \, r \, d\theta = w \quad (2.8)$$

where  $\theta_1$  is the value of  $\theta$  at the lower boundary and  $\theta_2$  is the value of  $\theta$  at the upper boundary.

Since the unknown variables in equation (2.4) are not unique therefore it requires an iterative solution with the condition it must satisfy continuity equation (2.8). To start the iteration some initial value of  $W$  is taken in equation (2.8) and then equation (2.4) is solved. This procedure is repeated with the new value of  $W$  until the correct solution is obtained.

## 2.2 FINITE DIFFERENCE APPROXIMATION

Finite difference approximation has been used for the solution of stream function  $u$ . For stream function solution a rectangular

grid has been established. Finite difference technique has to be applied at each node points of rectangular grid. Non-linear stream function equation

$$\frac{1}{r^2} \frac{\partial^2 u}{\partial \theta^2} + \frac{\partial^2 u}{\partial m^2} - \frac{1}{r^2} \frac{1}{\rho} \frac{\partial \rho}{\partial \theta} \frac{\partial u}{\partial \theta} + \left( \frac{\sin \alpha}{r} - \frac{1}{b \rho} \frac{\partial (b \rho)}{\partial m} \right) \frac{\partial u}{\partial m} = \frac{2b \rho \omega}{w} \sin \alpha$$

can be written for each node points to calculate unknown stream function throughout the region. The equations are nonlinear since the coefficients depend upon density. For n number of unknowns there are 'n' nonlinear equations. These nonlinear equations may be solved iteratively by successive over-relaxation as described in Ref. 16.

A typical mesh point with the numbering used to indicate the mesh points is shown in Fig. 2.5. The equation (1) can be approximated by

$$\begin{aligned} & \frac{2u_1}{h_1(h_1+h_2)} + \frac{2u_2}{h_2(h_1+h_2)} - \frac{2u_0}{h_1 h_2} + \frac{2u_3}{h_3(h_3+h_4)} + \frac{2u_4}{h_4(h_3+h_4)} - \frac{2u_0}{h_3 h_4} \\ & - \frac{1}{\rho_0} \left( \frac{\rho_2 - \rho_1}{h_1+h_2} \right) \left( \frac{u_2 - u_1}{h_1+h_2} \right) + \left( \frac{\sin \alpha_0}{r_0} - \frac{b_4 \rho_4 - b_3 \rho_3}{b_0 \rho_0 (h_4+h_3)} \right) \left( \frac{u_4 - u_3}{h_3 + h_4} \right) \\ & = \frac{2\omega}{w} b_0 \rho_0 \sin \alpha_0 \end{aligned} \quad (2.9)$$

where  $h_1 = r_0 (\theta)_1$

$h_2 = r_0 (\theta)_2$

The coefficients of  $u_i$  in equation (2.9) are calculated as follows.

$$u_0 = \sum_{i=1}^4 a_i u_i + k_0$$

where

$$a_{12} = \frac{2}{h_1 h_2} ; a_{34} = \frac{2}{h_3 h_4} ; a_0 = a_{12} + a_{34}$$

$$b_{12} = \frac{\rho_2 - \rho_1}{\rho(h_1 + h_2)} ; b_{34} = \frac{b_4 \rho_4 - b_3 \rho_3}{b_0 \rho_0 (h_3 + h_4)} - \frac{\sin \alpha_0}{r_0}$$

$$a_1 = \frac{1}{a_0 (h_1 + h_2)} \left( \frac{2}{h_1} + b_{12} \right) ; a_2 = \frac{a_{12}}{a_0} - a_1$$

$$a_3 = \frac{1}{a_0 (h_3 + h_4)} \left( \frac{2}{h_3} + b_{34} \right) ; a_4 = \frac{a_{34}}{a_0} - a_3$$

$$\text{and } k_0 = - \frac{2\omega}{w} \frac{b_0 \rho_0}{a_0} \sin \alpha_0 \quad (2.10)$$

The equations can be used at all interior mesh points and for mesh points adjacent to blade surfaces. Along the boundary the value of  $u$  is unknown, the equation will vary. Along upstream boundary  $\left( \frac{\partial u}{\partial \eta} \right)$  is known, and a finite difference approximation gives

$$u_0 = u_4 + h_4 \left( \frac{\partial u}{\partial \eta} \right)_{\text{inlet}} = u_4 + h_4 \left( \frac{\tan \beta_{\text{inlet}}}{S r_{\text{inlet}}} \right) \quad (2.11)$$

and along the downstream boundary

$$u_0 = u_3 + h_3 \left( \frac{\partial u}{\partial \eta} \right)_{\text{out}} = u_3 - h_3 \left( \frac{\tan \beta_{\text{out}}}{S r_{\text{out}}} \right) \quad (2.12)$$

The calculations of stream function along the boundary as shown in Fig. 2.6 can be derived by using periodic boundary conditions. Point '1' is outside the boundary. From the condition of periodicity

$$u_1 = u_{1,s} - 1$$

where point 1,s is above 1 at distance  $\theta$ . Substituting this condition in equation (2.10) gives

$$u_0 = a_1 u_{1,s} + \sum_{i=2}^4 a_i u_i - a_1 + k_0$$

The value of stream function  $u$  along MN, as shown in Fig. 2.7 is '1' greater than the corresponding value along AB. Thus

$$u_2 = u_{2-s} + 1$$

where point 2-s is distance 's' below MN in negative ' $\theta$ ' direction. Therefore substitution in equation (2.10) gives

$$u_0 = a_1 u_1 + a_2 u_{2-s} + a_3 u_3 + a_4 u_4 + a_2 + k_0 \quad (2.13)$$

The  $n$  equations are represented in the matrix form as

$$A\mathbf{u} = \mathbf{k} \quad (2.14)$$

where

$$\mathbf{u} = (u_1, u_2, \dots, u_n)^T$$

where all components are unknown values.

$A$  is the coefficient matrix of equation (2.10) to (2.13) and

$$\mathbf{k} = (k_1, k_2, \dots, k_{n-1}, k_n)^T$$

whose components are known constants.

The solution of equation (2.10) by iterative procedure is given by

$$u_i^{m+1} = u_i^m + \omega \left( - \sum_{j=1}^{i-1} a_{ij} u_j^{m+1} - \sum_{j=i+1}^n a_{ij} u_j^m + k_i - u_i^m \right) \quad (2.15)$$

for  $i = 1, 2, \dots, n$

where  $\omega$  is over-relaxation factor. The  $a_{ij}$  are the element of matrix A, and  $k_i$  are components of  $\underline{k}$ .

The optimum over-relaxation factor which maximizes the asymptotic rate of convergence can be expressed equivalently as

$$\omega = \frac{2}{1 + \sqrt{1 - \rho^2(\beta)}}$$

The above equation to determine optimum over-relaxation factor is derived in Ref. 16.

### 2.3 CALCULATION OF VELOCITY AND DENSITY

Once the values of stream functions are obtained using finite difference approximation, the derivatives  $\frac{\partial u}{\partial m}$  and  $\frac{\partial u}{\partial \theta}$  calculated. The relative velocity  $W$  is calculated using relationship

$$W^2 = W_m^2 + W_\theta^2$$

and for each new value of  $W$ ,  $W$  is calculated. The product  $W$  has its maximum value when  $W = W_{cr}$ . The relative velocity  $W$  has two values one is subsonic and the other one is supersonic. The subsonic values of relative velocity are calculated corresponding to the given values of  $W$  using Newton's method.

The thermodynamic relationships used in calculations are as follows.

$$\frac{T}{T'_{in}} = 1 - \frac{W^2 + 2\omega\lambda - (\omega r)^2}{2 C_p T'_{in}} \quad (2.16)$$

with the assumption of isentropic flow

$$\frac{p}{p'_{in}} = \left( \frac{T}{T'_{in}} \right)^{1/\nu - 1} \quad (2.17)$$

product  $pW$  is calculated as

$$pW = p'_{in} W \left( 1 - \frac{W^2 + 2\omega\lambda - (\omega r)^2}{2 C_p T'_{in}} \right)^{\frac{1}{\nu - 1}} \quad (2.18)$$

The derivative of above relation with respect to  $W$  is

$$\begin{aligned} \frac{\partial(pW)}{\partial W} = & - \frac{W^2 p'_{in}}{\nu R T'_{in}} \left( 1 - \frac{W^2 + 2\omega\lambda - (\omega r)^2}{2 C_p T'_{in}} \right)^{\frac{2-\nu}{\nu-1}} \\ & + p'_{in} \left( 1 - \frac{W^2 + 2\omega\lambda - (\omega r)^2}{2 C_p T'_{in}} \right)^{1/\nu - 1} \end{aligned} \quad (2.19)$$

The first value of relative velocity  $W$  is

$$W_0 = \frac{(pW)_{given}}{p_{inlet}} \quad (2.20)$$

The equation for the next value of  $W$  by Newton's method is

$$W_{n+1} = W_n + \frac{(pW)_{given} - p(W_n) W_n}{\left. \frac{\partial(pW)}{\partial W} \right|_{W = W_n}}$$

where  $n = 0, 1, 2, \dots$

#### 2.4 CALCULATION OF CRITICAL VELOCITY $W_{cr}$

$$W_{cr}^2 = \frac{2\gamma R}{\gamma + 1} T^* \quad (2.21)$$

$$\text{where } T^* = T'_{in} - \frac{2\omega\lambda - (\omega r)^2}{2 C_p} \quad (2.22)$$

#### 2.5 CALCULATION OF MAXIMUM VALUE OF MASS FLOW PARAMETERS $\dot{P}W$

The maximum value of mass flow is attained when  $W = W_{cr}$

$$(\dot{P}W)_{cr} = \dot{P}'_{in} W_{cr} \left( 1 - \frac{W_{cr}^2 + 2\omega\lambda - (\omega r)^2}{2 C_p T'_{in}} \right)^{1/\gamma - 1} \quad (2.23)$$

#### 2.6 CALCULATION OF LEADING EDGE, TRAILING EDGE RADII

If  $m^*$  and  $r^*$  are the co-ordinates of the centre of the arc then

$$(m - m^*)^2 + r^2 (\theta - \theta^*)^2 = R^2 \quad (2.24)$$

where  $R$  is the radius of leading or trailing edge.

#### 2.7 CALCULATION OF SURFACE LENGTH

The surface length of the blade is calculated by the relationship

$$\delta_n = \sum_{i=2}^n \sqrt{h_i^2 + (\theta_i - \theta_{i-1})^2 \left( \frac{r_i + r_{i-1}}{2} \right)^2} \quad (2.25)$$

#### 2.8 VELOCITY GRADIENT APPROACH

Velocity gradients are the lines that extend from one blade surface to another surface. The velocity gradient equation is

$$\frac{\partial W}{\partial \theta} = AW + B$$

An initial estimate of  $W$  on the lower boundary is available from the reduced weight flow solution. The initial velocity is obtained by dividing the reduced weight flow by reduced weight flow factor. A numerical solution to equation (2.4) is calculated by Runge-Kutta approach as follows:

If  $W_i$  is known at  $i^{\text{th}}$  point  $W_{i+1}$  is calculated by

$$W_{i+1}^* = W_i + (A_i W_i + B_i) (\theta_{i+1} - \theta_i)$$

$$W_{i+1}^{**} = W_i + (A_{i+1} W_{i+1}^* + B_{i+1}) (\theta_{i+1} - \theta_i)$$

$$\text{Then } W_{i+1} = \frac{W_{i+1}^* + W_{i+1}^{**}}{2}$$

The weight flow can be calculated by

$$W_{\text{est}} = \int_{\theta_1}^{\theta_2} W \cos \beta \, b r \, d\theta$$

The procedure is repeated until the calculated weight flow coincides with the actual weight flow.

## 2.9 AIRFOIL GEOMETRY

In the design of turbomachinery cascades, it is highly desirable that the curvature of the profile contour be continuous in order to avoid severe velocity changes Ref. 17 and 18. In cascade design it should be possible to introduce local changes without substantially affecting the remaining part of the profile. The airfoil profile is fitted by segments of  $n^{\text{th}}$  degree polynomials while maintaining continuous curvature variation.

The basic profile data for the design problem as shown in Fig. 2.8.  $S_2, S_3, S_4, P_2, P_3$  are suction and pressure surface defining points. A cartesian co-ordinate system is used with the Y-axis passing through the cascade leading edge and the x-axis through the centre of leading edge circle.

The governing equations for determining the polynomials are described by Z.Q.Ye in his paper Ref. 23. These equations are modified according to the requirement of TSONIC programme. The resulting equations are:

$$Y_{S1} = R_1 \sin \left( B_1^* - \frac{B_1^*}{2} \right)$$

$$X_{S1} = R_1 \left[ 1 - \cos \left( B_1^* - \frac{B_1^*}{2} \right) \right]$$

$$Y'_{S1} = \tan \left( \frac{\pi}{2} - B_1^* + \frac{B_1^*}{2} \right)$$

$$Y_{S3} = S_3 - (S \sin \beta + R_2) \cos (\bar{\Gamma} + B_2^*) - H$$

$$X_{S3} = B_x - (S \sin \beta + R_2) \cos (\bar{\Gamma} + B_2^*) - R_2$$

$$Y'_{S3} = \tan \left( \bar{\Gamma} + \beta_2^* - \frac{\pi}{2} \right)$$

$$Y_{S5} = -R_2 \sin \left( \beta_2^* - \frac{\beta_2^*}{2} \right) - H$$

$$X_{S5} = \beta_x - R_2 \left[ 1 - \cos \left( \beta_2^* - \frac{\beta_2^*}{2} \right) \right]$$

$$Y_{S5}^* = \tan \left( \beta_2^* - \frac{\beta_2^*}{2} - \frac{\pi}{2} \right)$$

$$Y_{P1} = -R_1 \sin \left( \beta_1^* + \frac{\beta_1^*}{2} \right)$$

$$X_{P1} = R_1 \left[ 1 + \cos \left( \beta_1^* + \frac{\beta_1^*}{2} \right) \right]$$

$$Y_{P1}^* = \tan \left( \frac{\pi}{2} - \beta_1^* - \frac{\beta_1^*}{2} \right)$$

$$Y_{P4} = -R_2 \sin \left( \beta_2^* + \frac{\beta_2^*}{2} \right)$$

$$X_{P4} = \beta_x - R_2 \left[ 1 + \cos \left( \beta_2^* + \frac{\beta_2^*}{2} \right) \right]$$

$$Y_{P4}^* = \tan \left( \beta_2^* + \frac{\beta_2^*}{2} - \frac{\pi}{2} \right)$$

In the design polynomials of degrees three and four are used to fit segments of the profile to the set of geometry conditions describing the cascade.

## 2.10 DETERMINATION OF INPUT FOR THE DESIGN

The cascade design can be initiated by selecting a pitch to axial chord ratio  $S/\beta_x$ , from loading considerations. The value of loading coefficient  $\psi_T$  is selected from design experience. From Horlock (25) the expression for  $\psi_T$  is given below

$$\psi_T = 2 \cdot \frac{S}{\beta_x} \sin^2 \beta_2 (\cot \beta_1 + \cot \beta_2)$$

Typical value for  $\psi_T$  may range from 0.6 to 1.2 with the final choice being determined by the satisfactory performance of the cascade.

A value of  $H$  can now be selected which determines the camber distribution and stagger of the airfoil. The cascade gaging angle ( $\beta_\lambda = \sin^{-1} (\tau/S)$ ) is determined from the given exit gas angle  $\beta_2$  and Mach number  $M_2$ . The gaging length or cascade throat is calculated from

$$\lambda = S \sin \beta_\lambda$$

The inlet metal angle  $\beta_1^*$  coincides with the inlet gas angle at zero incidence. The exit metal angle  $\beta_2^*$  and the uncovered turning  $\Gamma$  are finally decided on by finding an acceptable pressure distribution.

The wedge angles  $\Delta\beta_1^*$ ,  $\Delta\beta_2^*$  and the auxiliary points  $(x_{S2}, y_{S2})$ ,  $(x_{S4}, y_{S4})$ ,  $(y_{P2}, y_{P2})$ ,  $(x_{P3}, y_{P3})$  Fig. 2.8 on suction and pressure sides are determined in a trial and error procedure to give an acceptable airfoil shape. These variables strongly influence the cross channel area variation and hence the pressure distribution.

## CHAPTER 3

## COMPUTER PROGRAM

## 3.1 INTRODUCTION

The second degree nonlinear equations described in previous chapter are the governing equations for the blade to blade cascade flow and are solved by numerical methods using modern computers. Computer program for blade to blade flow have been developed by Katsanis in a series of publications Ref. 17,18,19 and 20. The latest version of Katsanis program is available in Ref. 21, published in 1969. The present program formulation is based on these publications of Katsanis. The program is further supplemented by using plot-10 facility available in DEC-1090 system at I.I.T.Kanpur. It is used to plot velocities, blade shapes, surface pressure distribution and to compare and modify airfoils with respect to existing airfoils.

The computer program requires geometrical parameters as input in  $m-\theta$  co-ordinates, appropriate gas constants and operating conditions such as inlet temperature and density, inlet and outlet flow angles, weight flow and rotational speed. Fig. 3.1 and Fig.3.2 show the  $m-\theta$  co-ordinate system for a typical blade to blade surface of revolution. The output obtained from the program includes stream function values throughout the blade to blade passage, streamline locations, blade surface velocities and velocity magnitude and directions at all interior mesh points.

The whole program is to run in two stages. In the first stage the solution of nonlinear finite difference equation is obtained through inner and outer iterations. Optimum value of over-relaxation factor is calculated for inner iteration to dampen the fluctuations and to lead the solution towards convergence. For each outer iteration the change in density is calculated and convergence of the solution is controlled by the variable Dentol (defined in input). The solution obtained through first stage for reduced weight flow is used as input for second stage to calculate the true velocities for actual weight flow with the help of velocity gradient technique.

### 3.2 DESCRIPTION OF INPUT DATA

The variables used as input are geometric and nongeometric. The geometrical input variables are shown in Fig. 3.1 and Fig. 3.2. The finite difference grid used in the program is shown in Fig. 3.3. All the input variables are described below.

AR - Gas constant J/kg/°K

BETAI - Inlet flow angle  $\beta_{te}$  with respect to meridional direction along BC

BETAO - Outlet flow angle  $\beta_{te}$  with respect to meridional direction along CF.

BETI1, BETI2 - Angles with respect to meridional direction at tangent points of leading and trailing edges radii with two blade surfaces, also  $\tan \beta = r (d\theta/dm)$  in degree.

- BETO1, BETO2 - Angles with respect to meridional direction at tangent points of trailing edge radii in degree.
- BESP - Array of stream channel normal thickness corresponding to MR and RMSP arrays in meters.
- CHORDF- Overall length in meridional direction, meters
- DENTOL- Tolerance in density per iteration for reduced weight flow
- GAM - Specific heat ratio
- MBI - Number of vertical mesh lines from AG to BG inclusive
- MBO - Number of vertical mesh lines from AH to CF inclusive
- MM - Total number of vertical meshlines in meridional direction from AH to DE.
- MR - Array of meridional 'm' co-ordinates of spline points for stream channel thickness, meters
- MSP1, MSP2 - Arrays of meridional 'm' co-ordinates of spline points on two blade surfaces, measured from the leading edge, meters.
- NBBI - Number of mesh spaces in 'θ' direction between AB and GH.
- NBL - Number of Blades
- NRSP - Number of spline points for stream channel radius (RMSP) and thickness (BESP) & co-ordinates.
- OMEGA- Rotational speed 'ω' rad/sec.
- ORF - Value of overrelaxation factor to be used in the solution of inner iteration
- RHOIP- Inlet stagnation density,  $\text{kg/m}^3$

REDFAC- Factor by which weight flow must be reduced in order to assure subsonic flow throughout the passage.

RI1, RI2-Leading edge radii of the two blade surfaces, meters

RO1,RO2 -Trailing edge radii of the two blade surfaces, meters

RMSP - Array of r-co-ordinates of spline points for the stream channel radii corresponding to MR array, meters.

STGRF - Angular  $\theta$ -co-ordinate for centre of trailing edge circle of blade with respect to the centre of leading edge circle of blade, radians

SPLNO1,SPLNO2 - Number of blade spline points given for each surface as input, include dummies points at leading and trailing edge.

TIP - Inlet stagnation temperature,  $^{\circ}\text{K}$

THSP1,THSP2 - Arrays of ' $\theta$ ' co-ordinates of spline points corresponding to MSP1 and MSP2, radians.

WTFL - Mass flow per blade for stream channel, kg/sec.

### 3.3 DESCRIPTION OF NORMAL OUTPUT

The output is controlled by the numerical values of various variables used within the program. A value of '0' for any of these variables will cause the output associated with the corresponding variables omitted. A value of '1' will cause the corresponding output to be printed for the final iteration. '2' for the first and final iterations; and '3' for all iterations.

- AANDK- Coefficient array constant vector and indexes of all adjacent points for each point in finite difference mesh.
- BLDAT- All geometrical information which is constant throughout the program (i.e. coordinates and first and second derivatives of all blade surface spline points, blade coordinates, blade slopes, blade curvature, radii and stream channel thickness, blade surface angles and slopes, ITV and IV arrays).
- ERSOR - Maximum change in stream function at any point for each iteration.
- INTVL - Velocity and flow angle at each interior mesh point for both reduced and actual weight flow.
- SLCRD - Streamline ' $\theta$ ' coordinates at each vertical mesh line
- STRFN - Value of stream function at each unknown mesh point in region
- SURVL - m co-ordinate, surface velocity, flow angle, distance along surface, and  $W/W_{cr}$  based on meridional velocity components.

### 3.4 OVERALL PROGRAM LOGIC

The computer program is composed of a main program and twenty seven subroutines. A list of these subroutines along with their functions is as follows:

1. INPUT - The subroutine reads all input data, calculates constants and initializes arrays.
2. PRECAL - This subroutine calculates all quantities which remain constant for a single problem.

3. COEF - This subroutine calculates the entries of the matrix  $A$  and the vector  $\underline{k}$ . These coefficients must be recalculated for each outer iteration.
4. SOR - It finds the linear solution to equation  $A\underline{u} = \underline{k}$  with fixed coefficients by the method of successive over-relaxation. It also estimates the optimum over-relaxation factor.
5. SLAX - It calculates the streamline locations and  $\int W_m$
6. TANG - It calculates  $\int W_\theta$  and then  $\int W$  and angle  $\beta$  throughout the region
7. VELOCY - It calculates the density  $\rho$  and velocity  $W$  throughout the region and on the blade surfaces
8. TVELCY - It solves the velocity gradient equation along each vertical line.
9. COEFBB - It computes the coefficients  $a_{ij}$  and constants  $k_i$  along a vertical mesh line from blade to blade
10. HRB - It calculates the values of  $h, r$ , and  $b$ .
11. AAK - It computes coefficients  $a_{ij}$  and the constants  $k_i$  at a single point.
12. BDRY12 - Subroutine BDRY12 is called by COEFBB. It alters the values of  $h$  and  $r$  calculated by HRB for point 1 or 2 (Fig. 1)
13. BDRY34 - Subroutine BDRY34 is called by COEFBB. It alters the values of  $h, r$  and  $b$  calculated by HRB for point 3 or 4 (Fig. 2.1).

14. SLAV - Subroutine SLAV calculates  $\frac{\partial u}{\partial \theta}$  and streamline locations. It also calculates  $\int W_m$  at each mesh point and  $\int W$  on blade surfaces.
15. VEL - The maximum relative change in density along a blade surface is calculated in VEL. It also calculates the value of density  $\rho$ , relative velocity  $W$  and ratio of  $W/W_{cr}$ .
16. BLCD - Subroutine BLCD calculates the  $\theta$ -co-ordinate and  $d\theta/dm$  of a blade surface for any given value of  $m$ .
17. IPF - Function IPF numbered the mesh point in the solution region.
18. VELGRA - It calculates the values of constants  $A$  and  $B$  to solve the velocity gradient equation.
19. MHORIZ - Subroutine MHORIZ calculates the  $m$ -co-ordinates of intersections of all horizontal mesh lines with a blade surface.
20. DENSITY- Subroutine DENSITY calculates the subsonic relative velocity  $W$  and corresponding density  $\rho$ , that result in a given value of the mass flow parameter  $\int W$ .
21. ROOT - Subroutine ROOT finds a root for  $f(x) = y$  by Newton's method.
22. SPLINE - It solves a tridiagonal matrix equation to obtain the coefficients for the piecewise cubic polynomial function giving the spline fit curve.

- 23. SPLN22 - It also solves the triadiagonal equation except that for the end conditions, the slopes are specified.
- 24. SPLINT - This subroutine is based on the cubic spline curve. The cubic spline curve is then used for interpolation.
- 25. SEARCH - It calculates the mass flow parameter  $\int W$  on blade surfaces.
- 26. CONTIN - CONTIN calculates a new estimate for the initial value of W for equation (2.4).
- 27. INTGRL - INTGRL calculator is the integral of a function passing through a given set of points.

An overall flow diagram for the program is given in Fig. 3.4. The overall control of the calculation procedure is maintained by the main routine.

## CHAPTER 4

### RESULTS AND DISCUSSION

The computer program discussed in the previous chapter is applicable to axial, mixed and radial flow turbines, since the effect of changes of cascade area in the flow direction and changes of radius are included in the program. However, in the present applications it has been applied for axial flow turbine cascade case only, including the rotor as well as stator cascade geometries. The test case have been chosen from Ref. 21 and 23. Initially considerable effort and time was devoted to obtain results similar to that of Ref. 22. This was necessary to validate the implementation of this program in the present investigations.

The airfoil is redesigned by selecting airfoil camber and thickness distributions. The application of computer graphic design methods by Z.Q. Ye (23) permits the designer to optimise the airfoil camber and thickness distribution, to minimize the suction surface rate of diffusion. The geometry redesign program is operated in an interactive mode by which the input geometric parameters are adjusted. To facilitate the initial specifications of a profile the few input parameters are initially set to zero. The cubical polynomial subprogram SPLINT is used to generate a pressure and suction surface blade profiles using the limited number of specified data. The profile is then successively modified by assigning values to the dummy points. Finally a profile is selected after several iterations, after obtaining the desired blade surface velocity distributions. The velocity distributions is normalised in terms

of critical velocity. The velocity distribution so obtained has lower suction surface peak velocity and the rate of diffusion between the location of velocity peak and the trailing edge is lower than that in the case of original profile. The uniformity in velocity distribution is also obtained.

#### TEST CASE I

For the first test case the design parameters for stator guide vanes were taken from Theodore Katsanis (21). The inlet and outlet flow angles assigned to stator guide vanes are '0' degree and '-67' degree respectively. The moderate flow has 0.36 and 1.05 MACH NUMBER at inlet and outlet respectively.

In the Fig. 4.1A the analytical results obtained through program are compared with the experimental results of J. Warren Whitney (22). There is a good agreement between the computed critical velocity ratio with the experimental data. There is some discrepancy near the trailing edge region of the suction surface. The numerical prediction methods are usually not so successful in predicting flow profiles in the vicinity of the blade leading and trailing edges.

In Fig. 4.1B the stator guide vane profile from Ref. 21 is shown by solid line. This profile is then modified by a systematic computational design system keeping all the thermodynamic parameters same. The modified profile is shown by dashed line. There is substantial change in the profile shape of the suction surface near

the trailing edge. The Fig. 4.2 displays the surface velocity distributions. The modified results have shown improvement over those of original blade profile particularly near the trailing edge region. Further the modified results are closer to the experimental data. The pressure coefficient curves in Fig. 4.3 shows similar improvement. This improvement over the blade surface is likely to minimize the profile losses and curb the tendency of separation on the suction surface.

## TEST CASE 2

In test case 2 for stator guide vane the geometrical input data are taken from Ye (23). The profile was assigned a loading coefficient of 0.8 with zero degree incidence and moderate subsonic exit flow ( $M_2 = 0.58$ ,  $M_{\max} = 0.62$ ). The exit flow angle is  $-55^\circ$ .

In Fig. 4.4 the stator guide vane profile is shown by solid line. The modified profile is shown by dashed line. It is displayed near the leading edge region for both the pressure and suction surfaces. The comparison of velocity ratio for both cases is shown in Fig. 4.5. The surface velocity variation in the original case of Res. 23 are smoothed in the modified design of the present case. Similar type of improvement seen in pressure coefficient distributions for both surfaces as shown in Fig. 4.6. Such an improved velocity distribution is likely to delay the separation on the suction surface.

## TEST CASE 3

Unlike the first two cases the test case 3 is the turbine rotor cascade redesign case. The rotor profile was assigned a loading coefficient of 0.94. The inlet and outlet flow angles are  $45.5^\circ$  and  $-68^\circ$  respectively. The moderate subsonic exit flow ( $M_2=0.74$ )

Fig. 4.7 is the computer generated graph of the turbine blade. There is substantially changes in camber and thickness distribution in case of modified profile particularly on the suction surface. There is a marginal reduction in the blade profile thickness in the modified case. The velocity distribution for both cases are shown in Fig. 4.8. The velocities obtained through modified profile for turbine blade show a good improvement over previous case. On the suction surface the peak velocity is lower in the modified design and also more uniform velocity distribution is obtained in the trailing edge region. Likewise the pressure coefficient distribution along the profiles are shown in Fig. 4.9. The modified results indicate the refinement of pressure coefficient distribution over previous one and reduce the possibility of early separation because the minimum pressure level is higher.

#### 4.1 CONCLUSIONS

The first part of this work consisted of an implementation of the TSONIC program for blade to blade calculations, given in Ref. 21. Since this program in Ref. 21 has been developed after successive modifications over previous programs given in Ref. 17, 18, 19 and 20. Initially substantial time and effort was spent in organising and implementing it. The results presently obtained were checked with the results given in Ref. 21 for the standard test case of stator blade row. After complete agreement was obtained in the two cases, other test cases were taken up.

In the second part of the work a systematic computational design system was used, rapid and effective redesign of existing blade profiles turbine cascades. The approach followed was similar to that of Ye. The modified profiles thus obtained after several iterations show improvement over original ones in respect of blade surface velocity distribution and are likely to encounter reduced profile losses.

#### 4.2 SCOPE OF FUTURE WORK

In the present work efforts are made to modify the blade profile in order to reduce the profile losses. Due to limitations of time however the effect of losses on surface velocity distribution has not been included in the program. This can be done by using a boundary layer analysis program. A program for reanalysis of leading and trailing edge velocity distribution can also be incorporated to obtain more accurate results near the leading and trailing edge region|

## REFERENCES

1. Chaplygin S.A. 'Theory of cascade wing Math. Journ. Vol. XXIX (1913)'.
2. Erwin, I.H. and Yacobi, L.A. 'Method of estimating the incompressible flow pressure distribution of compressor blade sections at design angle of attack', NACA R and M L53F17 (1953).
3. Wu Chung Hua and Brown, C.A., 'Method of analysis for compressible flow past arbitrary turbomachine blades on general surfaces of revolution', NACA TN 2407 (1959).
4. Theodorsen, T., 'Theory of wing sections of arbitrary shape', NACA Rep. 411 (1931).
5. Marsh, H., 'A digital computer program for the through-flow fluid mechanics on an arbitrary turbomachine using a matrix method', ARC F&M 3509 (1968).
6. Habshi, W.G., Dueck, E.G. and Kenny, D.P. 'Finite element approach to compressor blade to blade cascade analysis', AIAA J, 17,7 p. 693 (1979).
7. Adler, D. and Krimerman, Y., 'Comparison between the calculated subsonic inviscid three dimensional flow in a centrifugal impeller and measurements', ASME Symp, Perf. Pred. Centrif. pumps and Comp. p. 19 (1980).
8. McDonald, P.W., 'The computation of transonic flow through two dimensional gas turbine cascades', ASME Paper 71-GT 89 (1971).

9. Denton, J.D. 'A time marching method for two and three dimensional blade to blade flows', ARC R and M 3775 (Oct. 1974).
10. Kurzrock, J.W. and Novick, A.S., 'A transonic flow around rotor blade elements', ASME paper 75 FE-24 (1975).
11. Jansen, W. 'A method for calculating the flow in a centrifugal impeller', Unpublished N.R.E.C. Report.
12. Bindon, J.P. and Carmichael, A.D. 'Streamline curvature analysis of compressible and high Mach Number cascade flows', Proc. I.Mech. E (1970).
13. Katsanis, T. 'Use of arbitrary quasi-orthogonals for calculating flow distribution in the meridional plane of a turbomachine', NASA TND-2546 (1964).
14. Wilkinson, D.H. 'Stability convergence and accuracy of two-dimension streamline curvature methods using quasi-orthogonals' I.Mech.E. Thermodynamics and Fluid Mechanics Convention, Paper 35 (1970).
15. Katsanis, Theodore and Dellner, Lois T., 'A quasi-three dimensional method for calculating blade surface velocities for an axial flow turbine blade. NASA TMX-1394, 1967.
16. Varga, Richard S., 'Matrix iterative analysis' Prentice-Hall Inc. 1962.
17. Katsanis, Theodore, and Dellner, Lois T., 'A quasi-three-dimensional method for calculating blade surface velocities for an axial flow turbine blade', NASA TMX-1394, 1967.

18. Katsanis, Theodore, 'Computer program for calculating velocities and streamlines on a blade to blade stream surface of a turbo-machine', NASA TND-4525, 1968.
19. Katsanis, Theodore, and McNally, William D., 'Revised Fortran program for calculating velocities and streamlines on a blade-to-blade stream surface of a turbomachine', NASA TMX-1764, 1969.
20. Katsanis, Theodore, and McNally, William D. 'Fortran program for calculating velocities and streamline on blade-to-blade stream surface of a Tandem blade turbomachine', NASA TND-5044, 1969.
21. Katsanis, Theodore, 'Fortran program for calculating transonic velocities on a blade to blade stream surface of a turbomachine', NASA TND-5427, 1969.
22. Whitney, Warren J., Szanca, Edward M., Moffitt, Thomas P., and Monroe, Daniel E., 'Cold air investigation of a turbine for high temperature engine application, I. Turbine design and overall stator performance' NASA TND-3751, 1967.
23. Ye, Z. Q. 'A systematic computational design system for turbine cascades, airfoil geometry, and blade to blade analysis.' ASME Journal Vol. 106, July, 1984.
24. Monello, J.A., Mitchell, W.S. and Tall, W.A. 'Application of non-series airfoil design technology to highly loaded turbine exit guide vanes' ASME Journal of Engineering for Power, Vol. 101, 1979, pp. 202-211.
25. Horlock, J.H. 'Axial flow turbines', BUTTERWORTHS, 1966

## APPENDIX 'A'

## DERIVATION OF VELOCITY GRADIENT EQUATION

The velocity-gradient equation is an expression of the force equation. By a balance of force in the  $\theta$ -direction, the following equation can be obtained.

$$\frac{\partial W}{\partial \theta} = \frac{1}{W} \frac{d(rV_{\theta})}{dt} = \frac{1}{W} \frac{d(rW_{\theta} + \omega r^2)}{dt} \quad (A1)$$

The time derivative indicates the change in the quantity for a moving particle as a function of time. We make use of the following relations (Fig. 2.1)

$$W_{\theta} = W \sin \beta$$

$$W_m = W \cos \beta$$

$$W_r = W_m \sin \alpha$$

$$W_z = W_m \cos \alpha$$

$$\frac{dr}{dt} = W_r$$

$$r \frac{d\theta}{dt} = W_{\theta}$$

$$\frac{dm}{dt} = W_m$$

$$\frac{ds}{dt} = W$$

$$\frac{dB}{dt} = W \frac{dB}{ds}$$

$$\frac{dW}{dt} = W_{\theta} \frac{\partial W}{r \partial \theta} + W_m \frac{\partial W}{\partial m}$$

We can perform the indicated differentiation of the right side of equation (A1) by using the preceding relations, and then solve for  $\partial W / \partial \Theta$  (which appears on both sides of the equation) to obtain

$$\frac{\partial W}{\partial \Theta} = W \left( \frac{r}{\cos \beta} \frac{d\beta}{ds} + \sin \alpha \tan \beta \right) + r \tan \beta \frac{\partial W}{\partial m} + 2\omega r \frac{\sin \alpha}{\cos \beta} \quad (A2)$$

We desire now to evaluate  $d\beta/ds$  in terms of first and second derivatives of  $\Theta$  with respect to  $m$  along streamlines. The following relations hold for streamlines.

$$\tan \beta = \frac{r d\Theta}{dm} \quad (A3)$$

$$\tan \beta = \frac{W_\Theta}{W_m} = - \frac{r \frac{\partial u}{\partial m}}{\frac{\partial u}{\partial \Theta}} \quad (A4)$$

Equation (A4) is obtained by using equations (2.2) and (2.3). Also along streamlines we have

$$\frac{dm}{ds} = \cos \beta \quad (A5)$$

$$\frac{dr}{dm} = \sin \alpha \quad (A6)$$

Now differentiate equation A3) and use equations (A5) and (A6) to obtain

$$\frac{d\beta}{ds} = r \cos^3 \beta \frac{d^2 \Theta}{dm^2} + \frac{\sin \alpha \sin \beta \cos^2 \beta}{r} \quad (A7)$$

Along the surface of the blade  $d^2 \Theta / dm^2$  can be easily calculated since  $\Theta$  is given explicitly as a function  $m$ . However, in the passage  $d^2 \Theta / dm^2$  is given indirectly by the stream function. Hence we will need an expression for  $d^2 \Theta / dm^2$  in terms of the partial

derivatives of the stream function. First, from equation (A3) and (A4) we have

$$\frac{d\theta}{dm} = - \frac{\partial u / \partial m}{\partial u / \partial \theta} \quad (A8)$$

By differentiating equation (A8) we obtain

$$\frac{d^2\theta}{dm^2} = \frac{\partial}{\partial m} \left( - \frac{\partial u}{\partial \theta} \right) + \frac{\partial}{\partial \theta} \left( - \frac{\partial u}{\partial m} \right) \frac{d\theta}{dm} = 2 \frac{\partial u}{\partial \theta} \cdot \frac{\partial u}{\partial m} \frac{\partial^2 u}{\partial \theta \partial m} - \left( \frac{\partial u}{\partial \theta} \right)^2 \frac{\partial^2 u}{\partial m^2} - \left( \frac{\partial u}{\partial m} \right)^2 \frac{\partial}{\partial \theta} \frac{1}{(\partial u / \partial \theta)^3} \quad (A9)$$

Finally by using the fact (from eqs. (A3) and (A8)) that

$$\frac{r \cos \beta}{\partial u / \partial \theta} = - \frac{\sin \beta}{\partial u / \partial m}$$

We can obtain

$$r^2 \cos^2 \beta \frac{\partial^2 \theta}{\partial m^2} = \sin^2 \beta \left[ \frac{\partial^2 u}{\partial \theta \partial m} - \frac{\frac{\partial u}{\partial \theta}}{\left( \frac{\partial u}{\partial m} \right)^2} \frac{\partial^2 u}{\partial m^2} - \frac{\frac{\partial^2 u}{\partial \theta^2}}{\frac{\partial u}{\partial \theta}} \right] \quad (A10)$$

By using equations (A7) and (A10), equation (A2) can be put in the following form :

$$\frac{\partial W}{\partial \theta} = AW + B \quad (A11)$$

where

$$A = r^2 \cos^2 \beta \frac{d^2 \theta}{dm^2} + \sin \alpha \tan \beta (1 + \cos^2 \beta) \quad (A12a)$$

is used on blade surface,

$$A = \sin^2 \beta \left[ 2 \frac{\frac{\partial^2 u}{\partial \theta \partial m}}{\frac{\partial u}{\partial m}} - \frac{\frac{\partial u}{\partial \theta}}{(\frac{\partial u}{\partial m})^2} \frac{\frac{\partial^2 u}{\partial m^2}}{\frac{\partial u}{\partial \theta}} - \frac{\frac{\partial^2 u}{\partial \theta^2}}{\frac{\partial u}{\partial \theta}} \right] + \sin \alpha \tan \beta (1 + \cos^2 \beta) \quad (A12b)$$

is used at interior points and

$$B = r \tan \beta \frac{\partial W}{\partial m} + 2 \omega r \frac{\sin \alpha}{\cos \beta} \quad (A13)$$

Equations (A11) to (A13) are in the form used in the program.

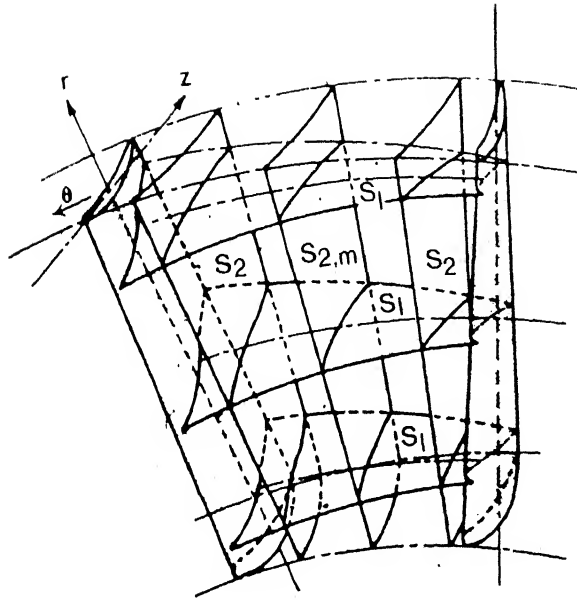


FIG 1.1 SCHEMATIC VIEW OF BLADE TO BLADE PLANE  $S_1$  AND MERIDIONAL PLANE  $S_2$ .

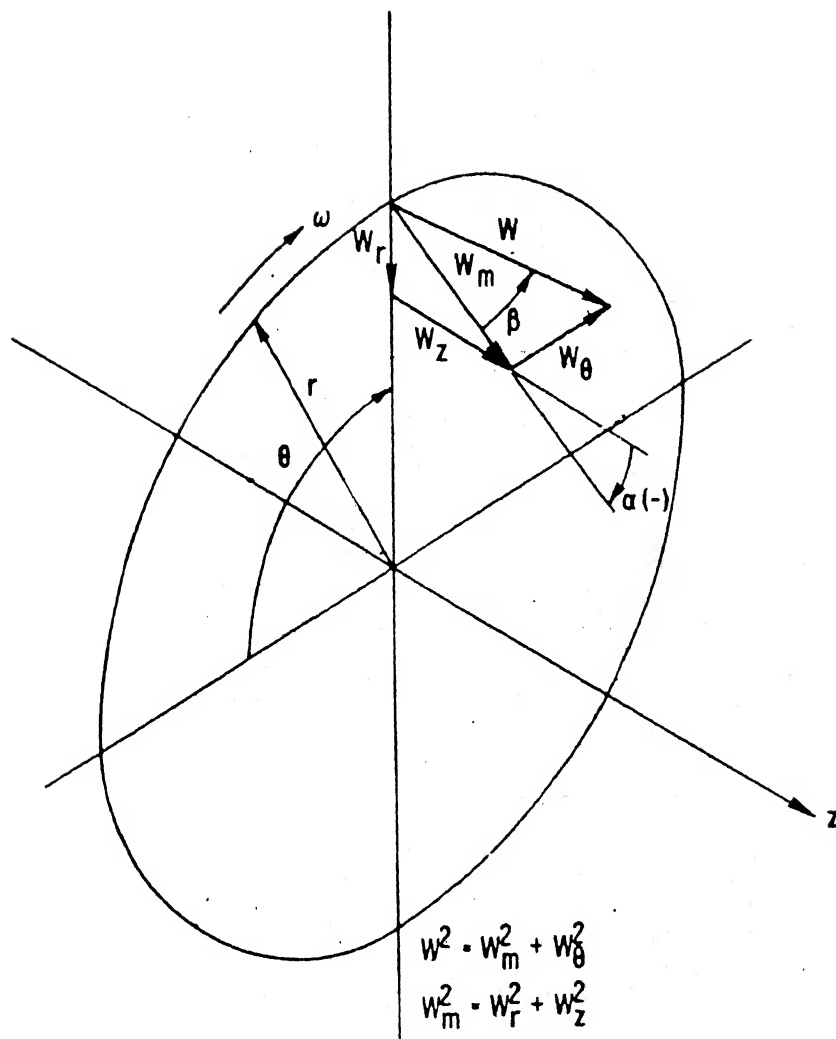


FIG 2.1 CYLINDRICAL CO-ORDINATE SYSTEM AND VELOCITY COMPONENTS.

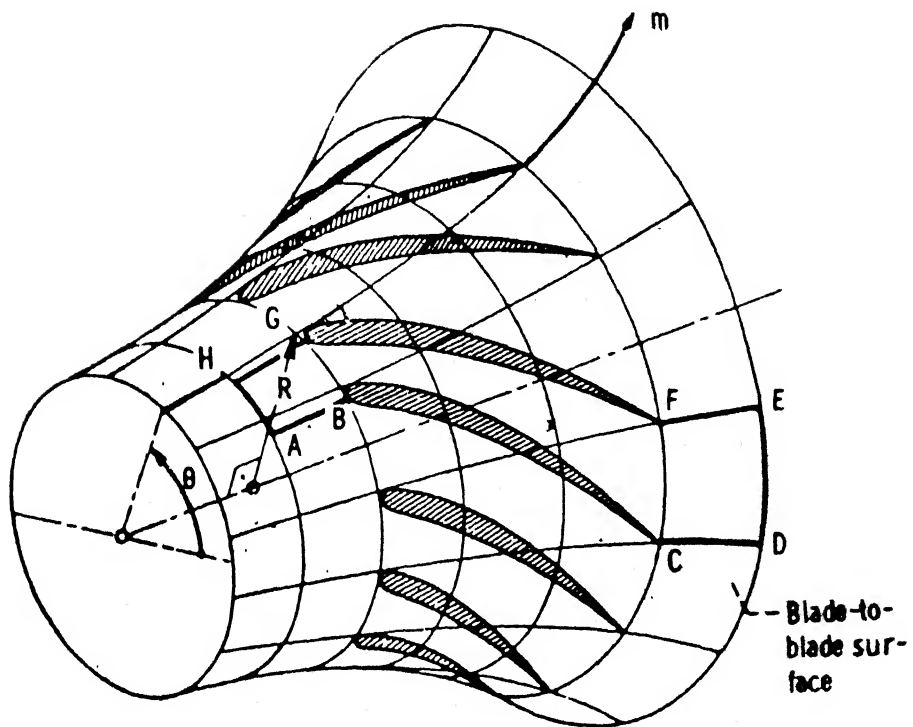


FIG 2.2 BLADE TO BLADE SURFACE OF REVOLUTION  
SHOWING  $m-\theta$  CO-ORDINATES

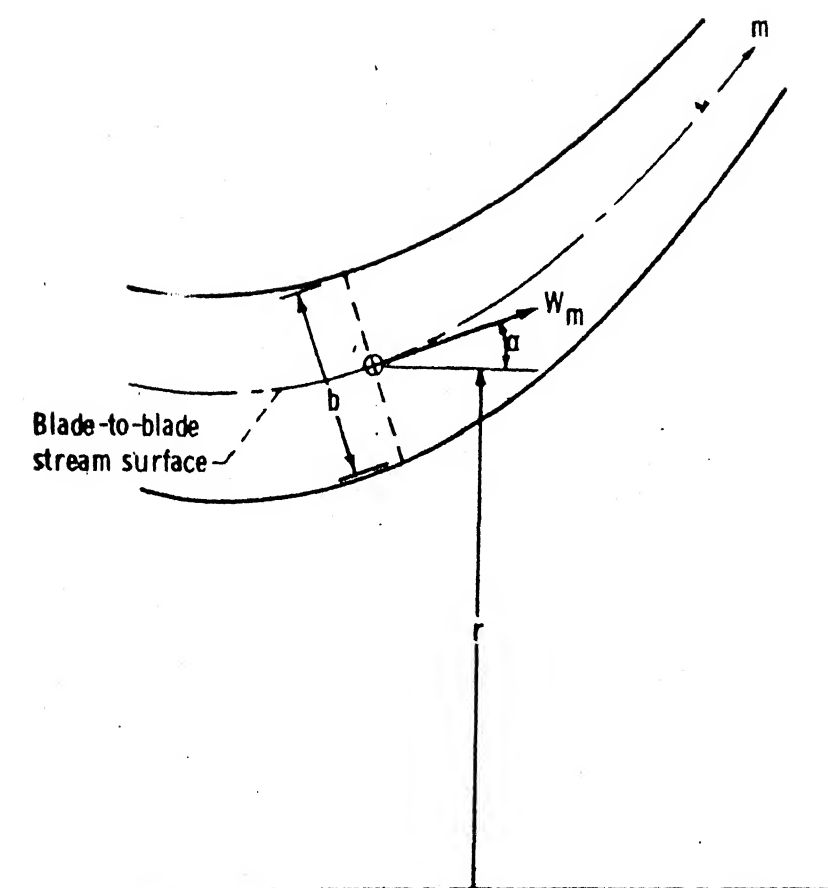


FIG 2.3 FLOW IN A MIXED FLOW STREAM CHANNEL

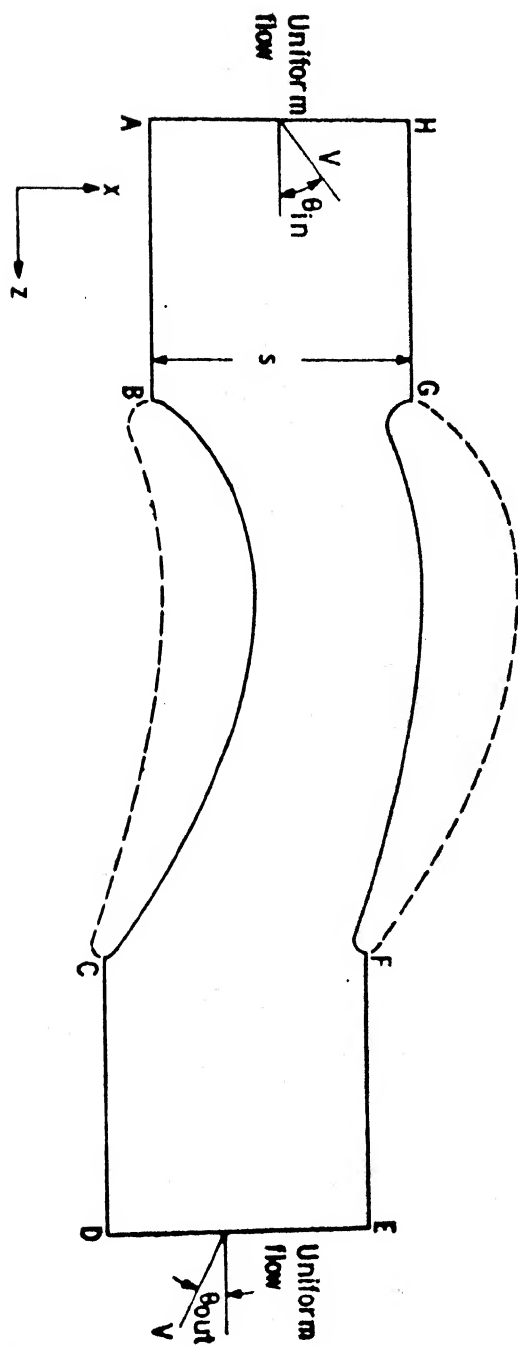


FIG 2.4 FINITE FLOW REGION OF TURBINE CASCADE

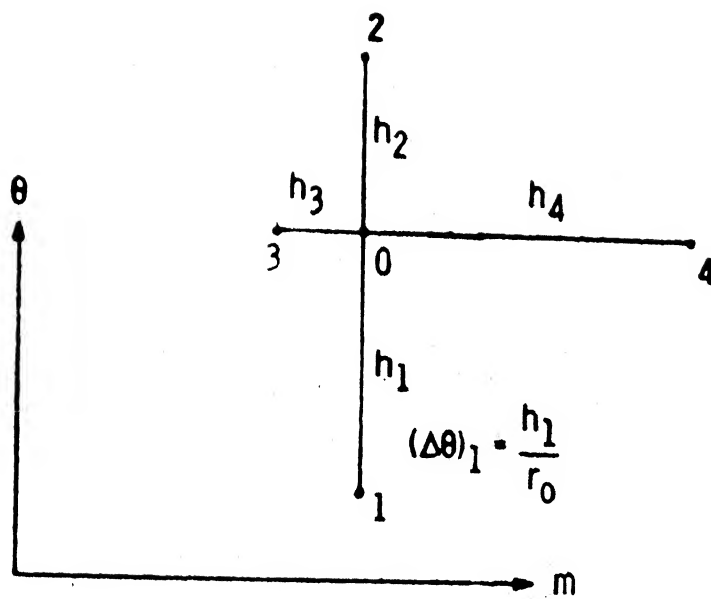


FIG 2.5 NOTATION FOR ADJACENT MESH POINTS AND MESH SPACES.

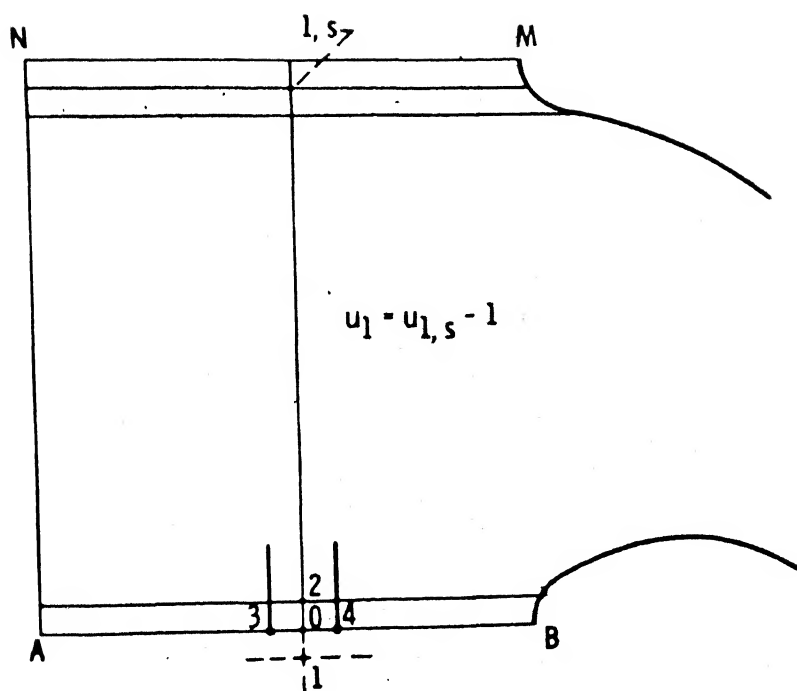


FIG 2.6 MESH POINTS ON LOWER BOUNDARY.

CENTRAL LIBRARY  
I. I. T., Kanpur.

Acc. No. **A** 97968

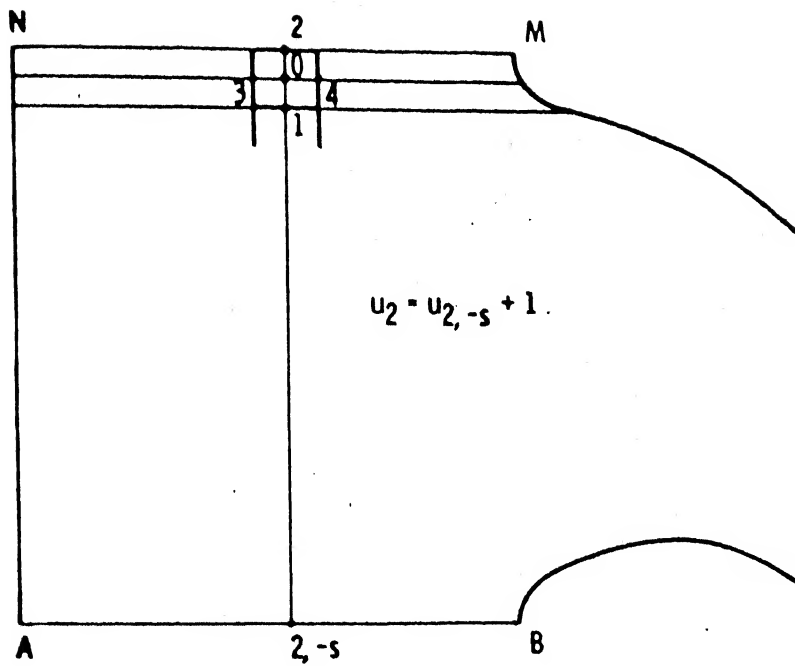


FIG 2.7 MESH POINTS ON UPPER BOUNDARY.

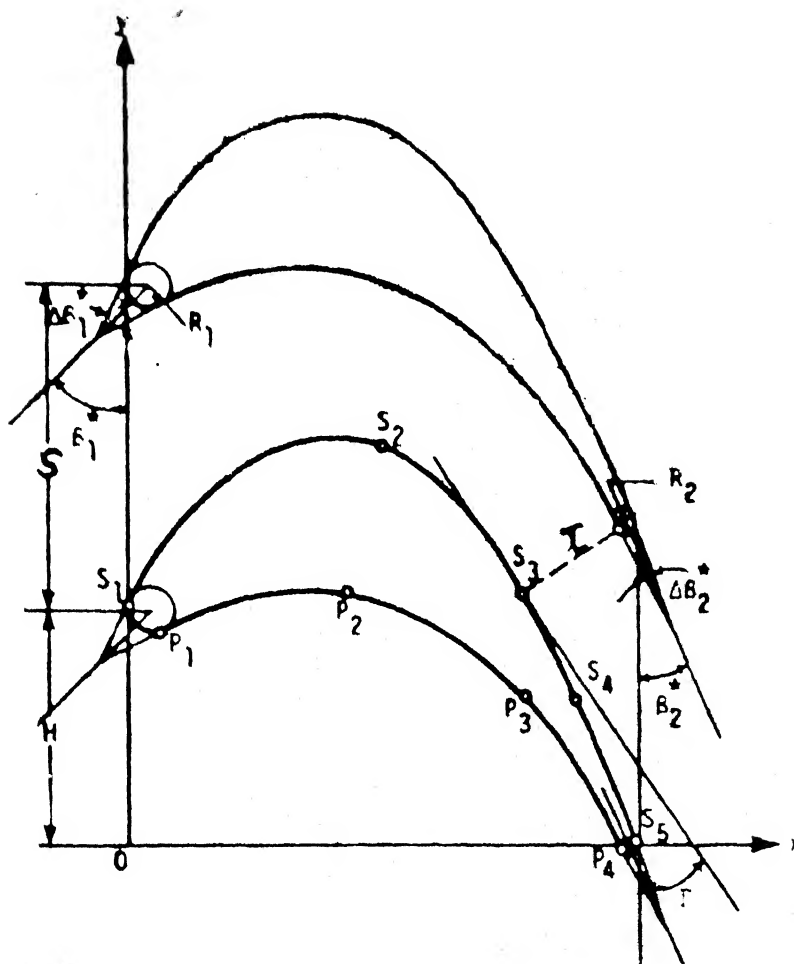


FIG 2.8 CO-ORDINATE SYSTEM AND CASCADE GEOMETRIC PARAMETERS.

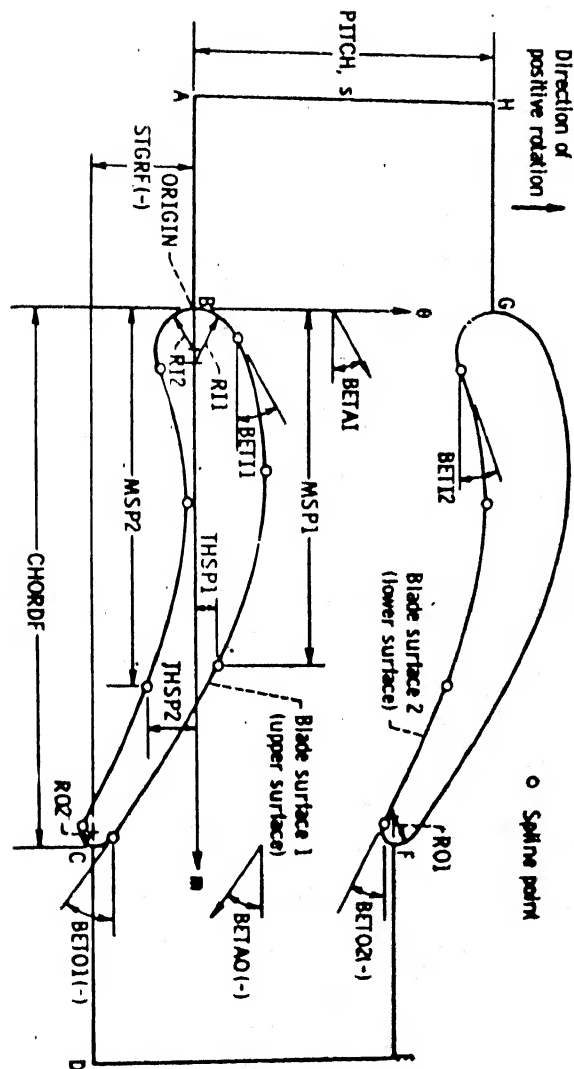


FIG 3.1 GEOMETRIC INPUT VARIABLES ON BLADE TO BLADE  
STREAM SURFACE.

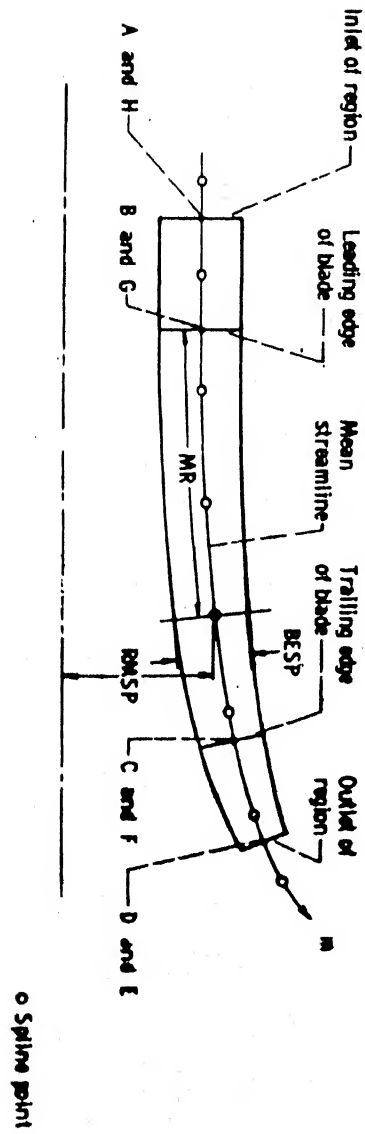


FIG 3.2 GEOMETRIC INPUT VARIABLES DESCRIBING STREAM CHANNEL  
IN MERIDIONAL PLANE.

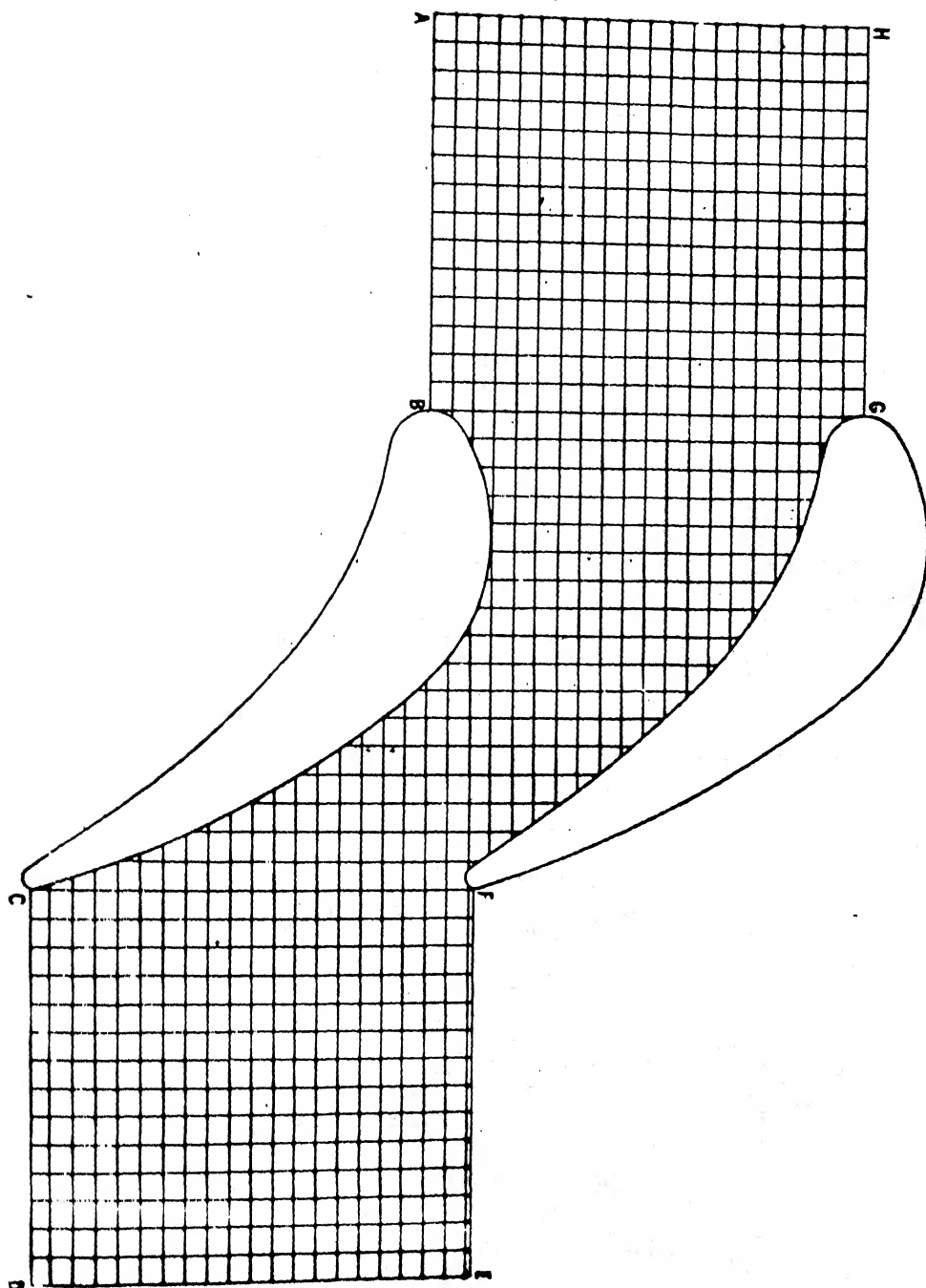


FIG 3.3 FINITE DIFFERENCE MESH IN BLADE TO BLADE SOLUTION REGION.

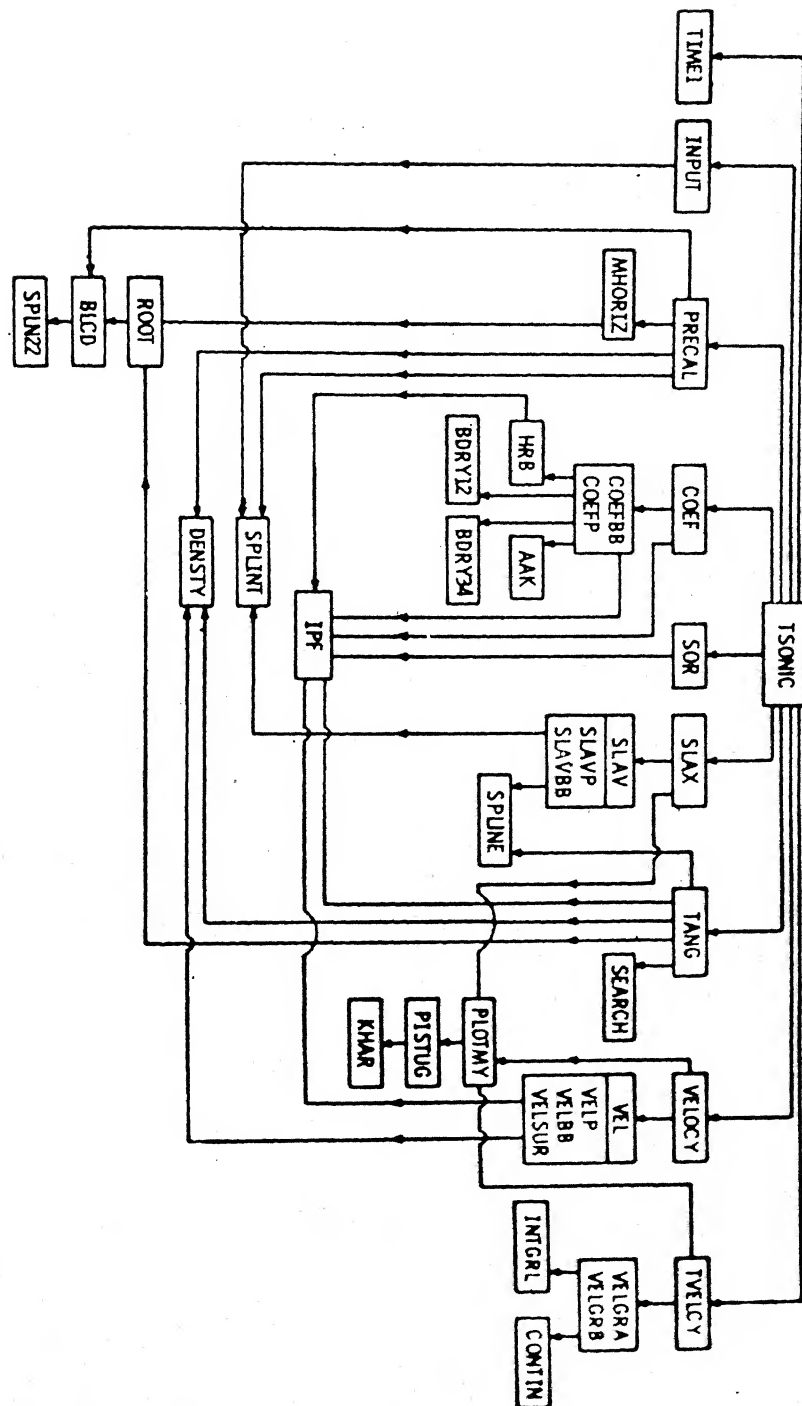


FIG 3.4 FLOW CHART FOR SUBROUTINE CALLING SEQUENCE.

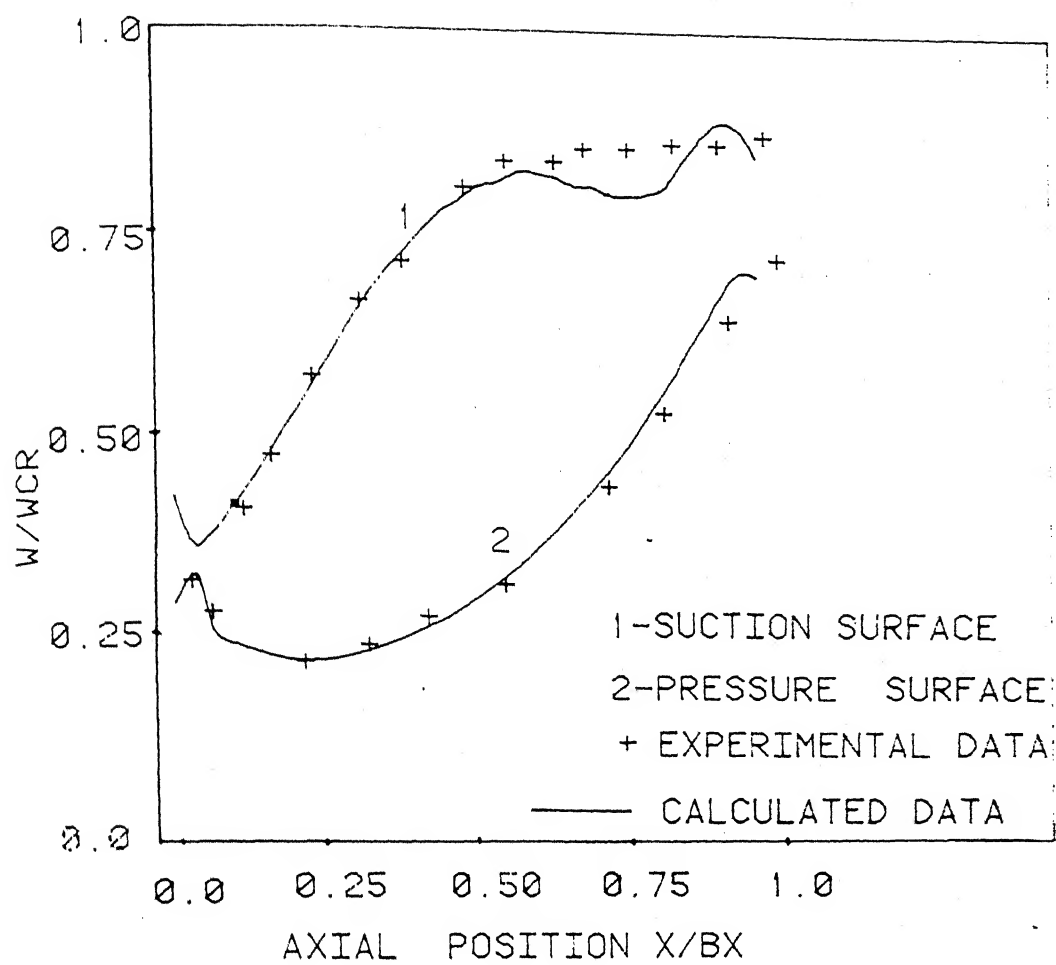


FIG.4.1A COMPARISON OF BLADE SURFACE  
VELOCITIES WITH EXPERIMENTAL DATA  
FOR STATOR CASE

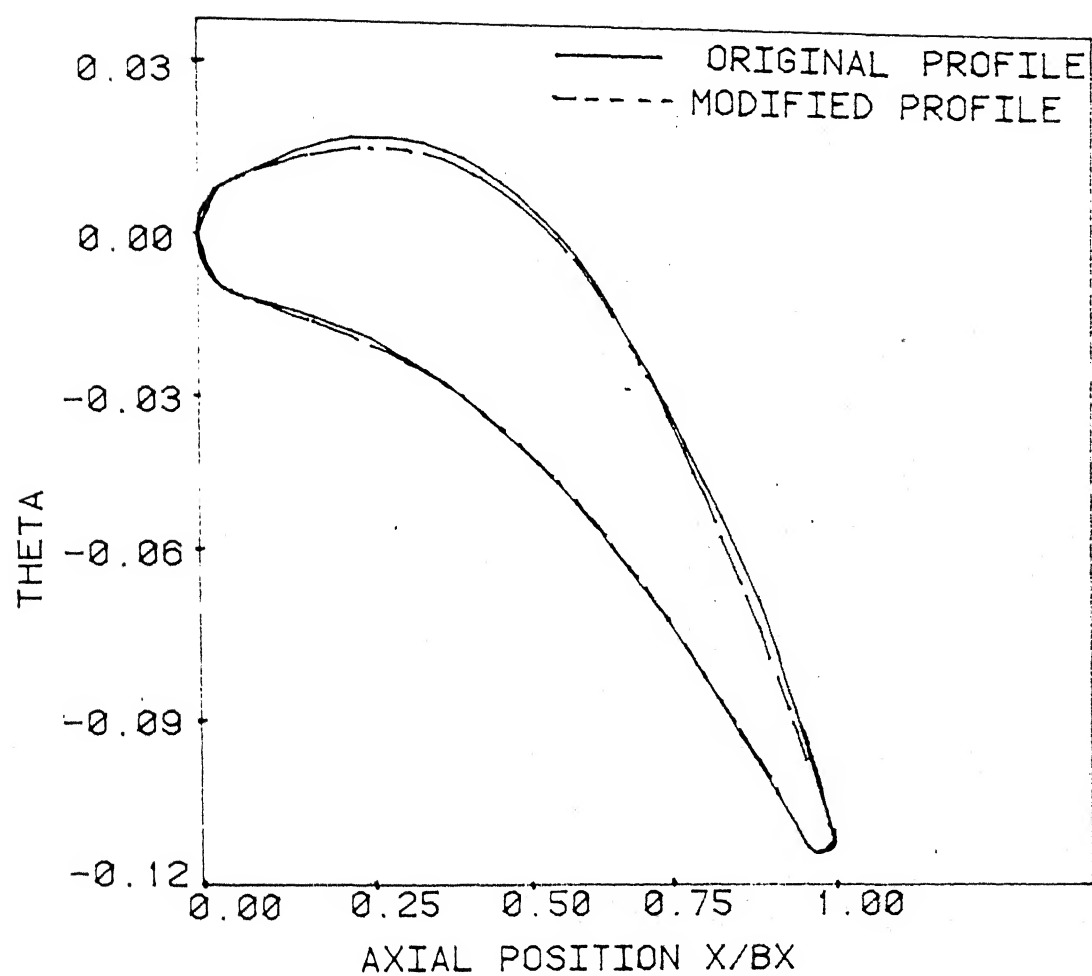


FIG.4.1B COMPARISON OF BLADE PROFILE

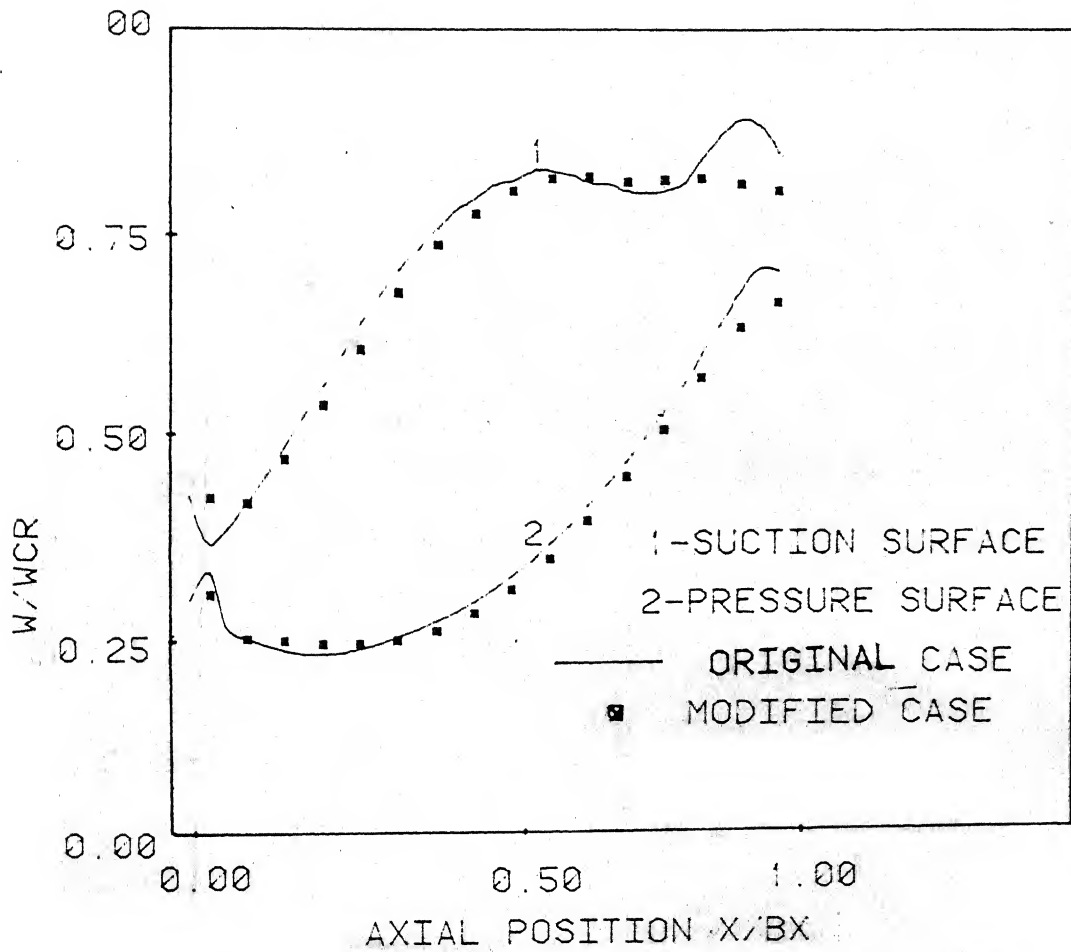


FIG 4.2 COMPARISON OF BLADE SURFACES VELOCITY

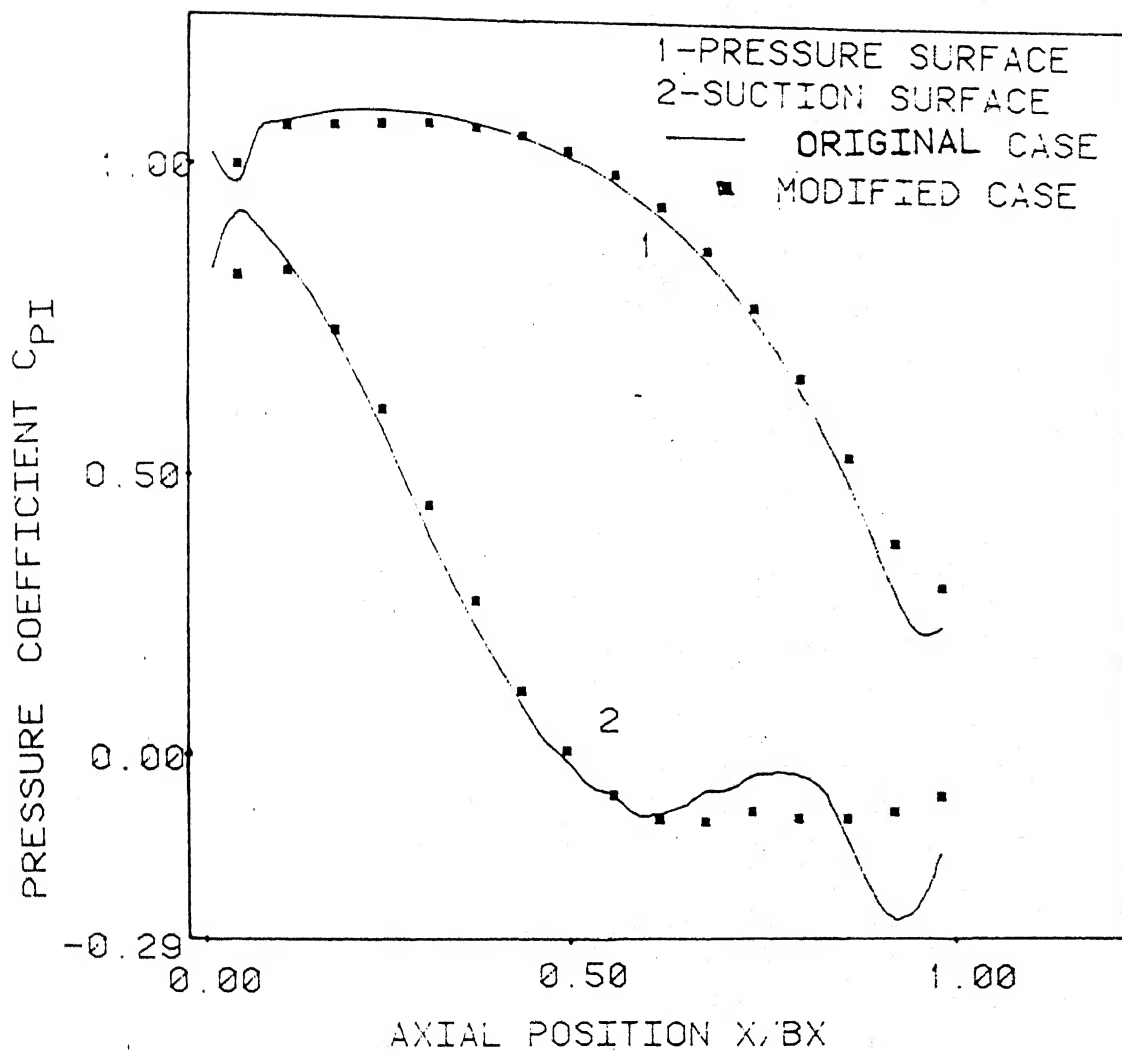


FIG 4.3 COMPARISON OF SURFACE PRESSURE COEFFICIENT DISTRIBUTION

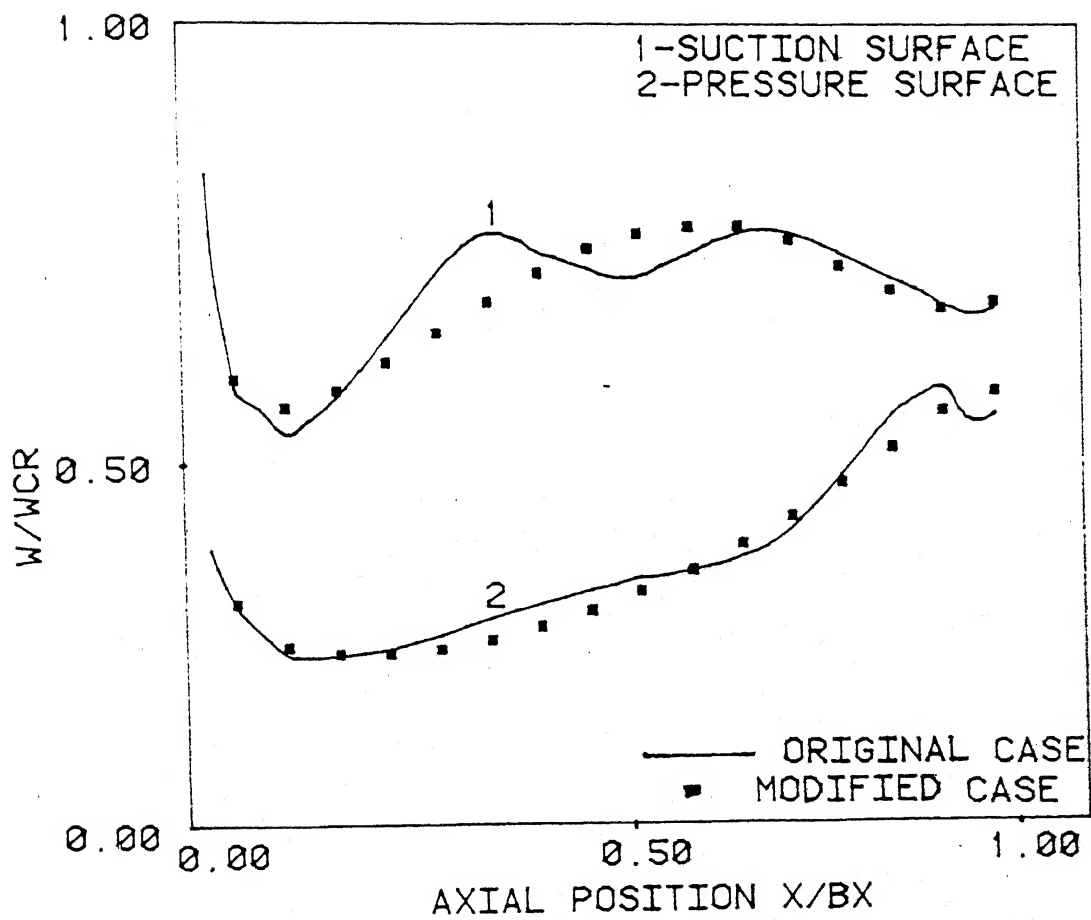


FIG 4.5 COMPARISON OF BLADE SURFACE  
VELOCITY FOR STATOR GUIDE VANE

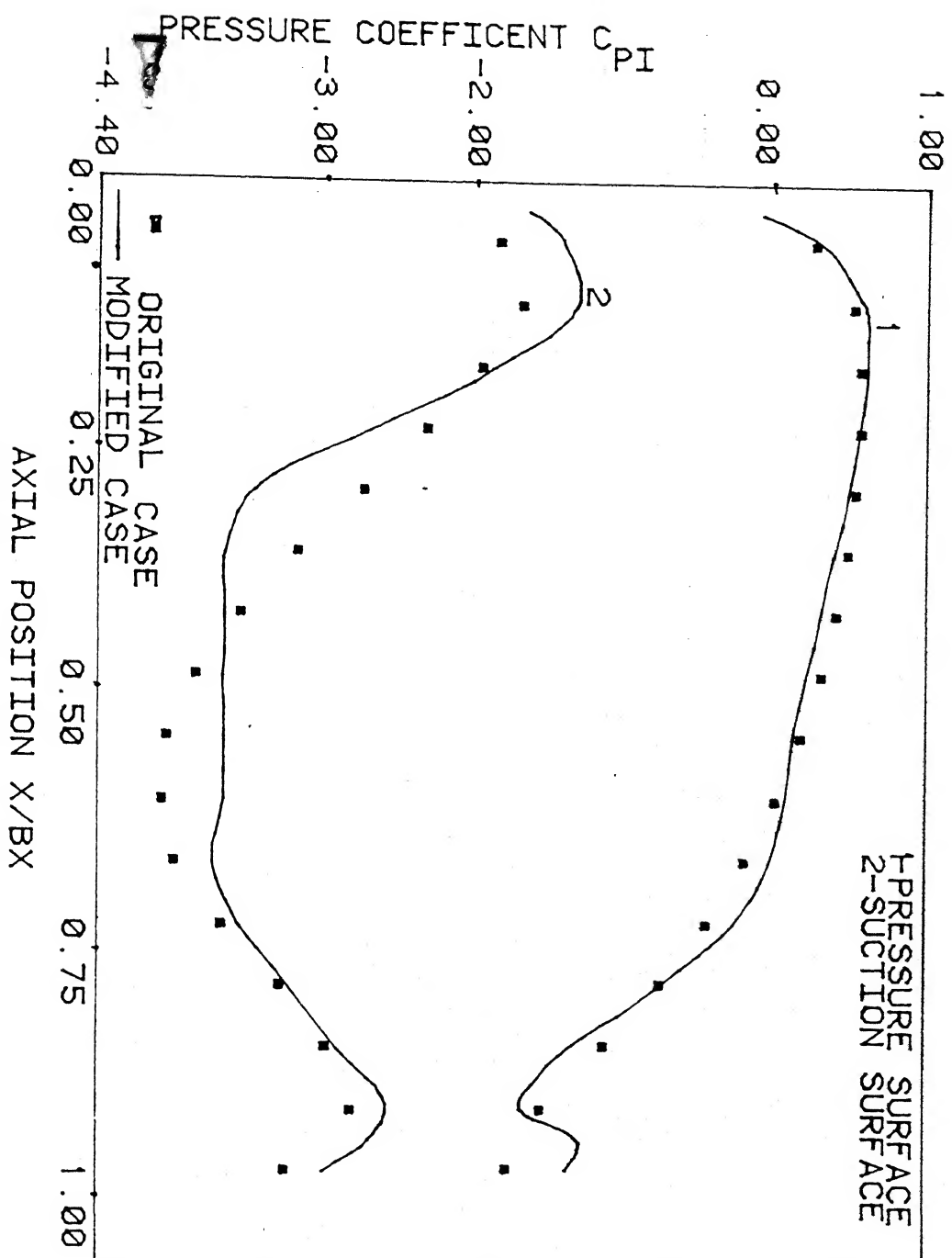


FIG 4.6 COMPARISON OF SURFACES PRESSURE COEF.  
DISTRIBUTION FOR STATOR GUIDE VANE

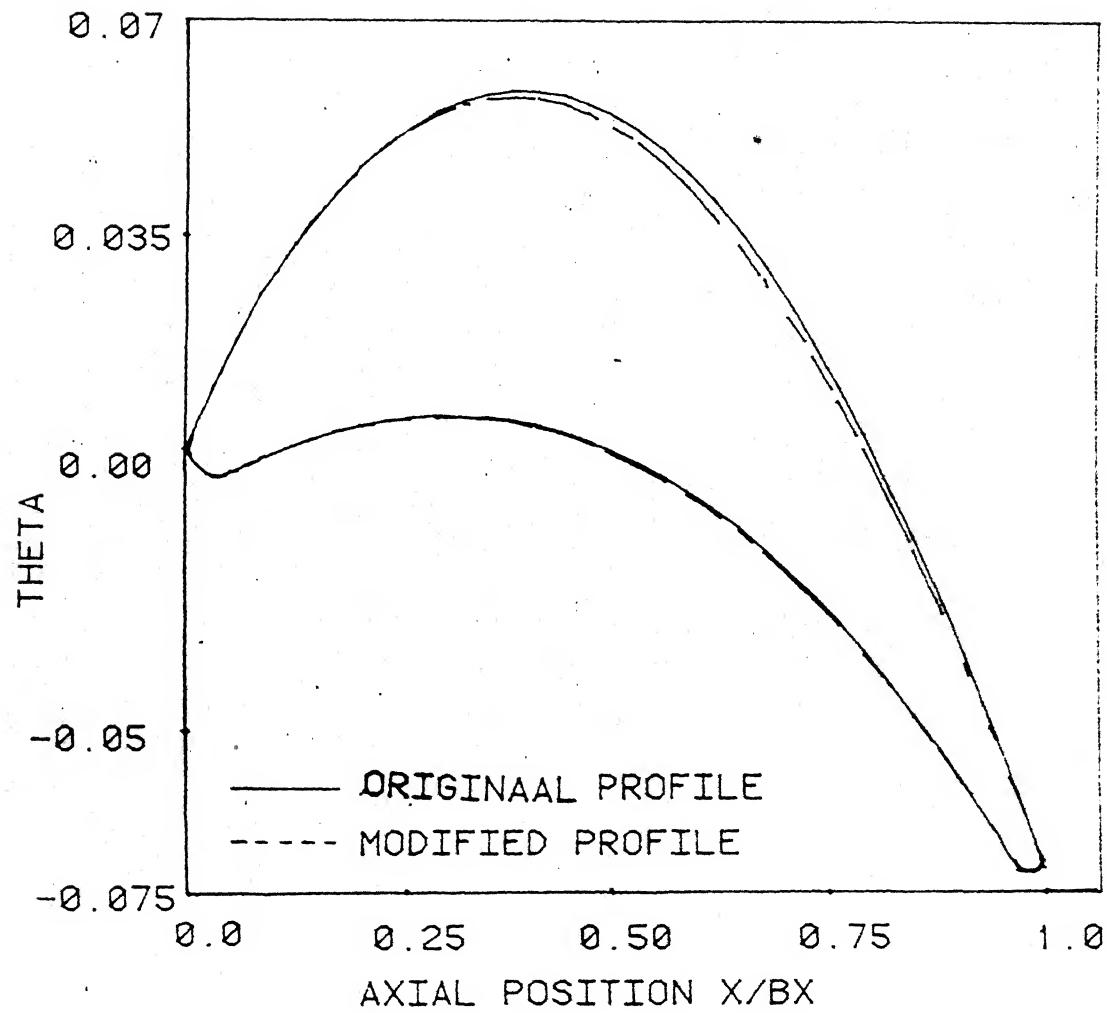


FIG 4.7 COMPARISION OF BLADE PROFILE  
FOR TURBINE ROTOR CASE

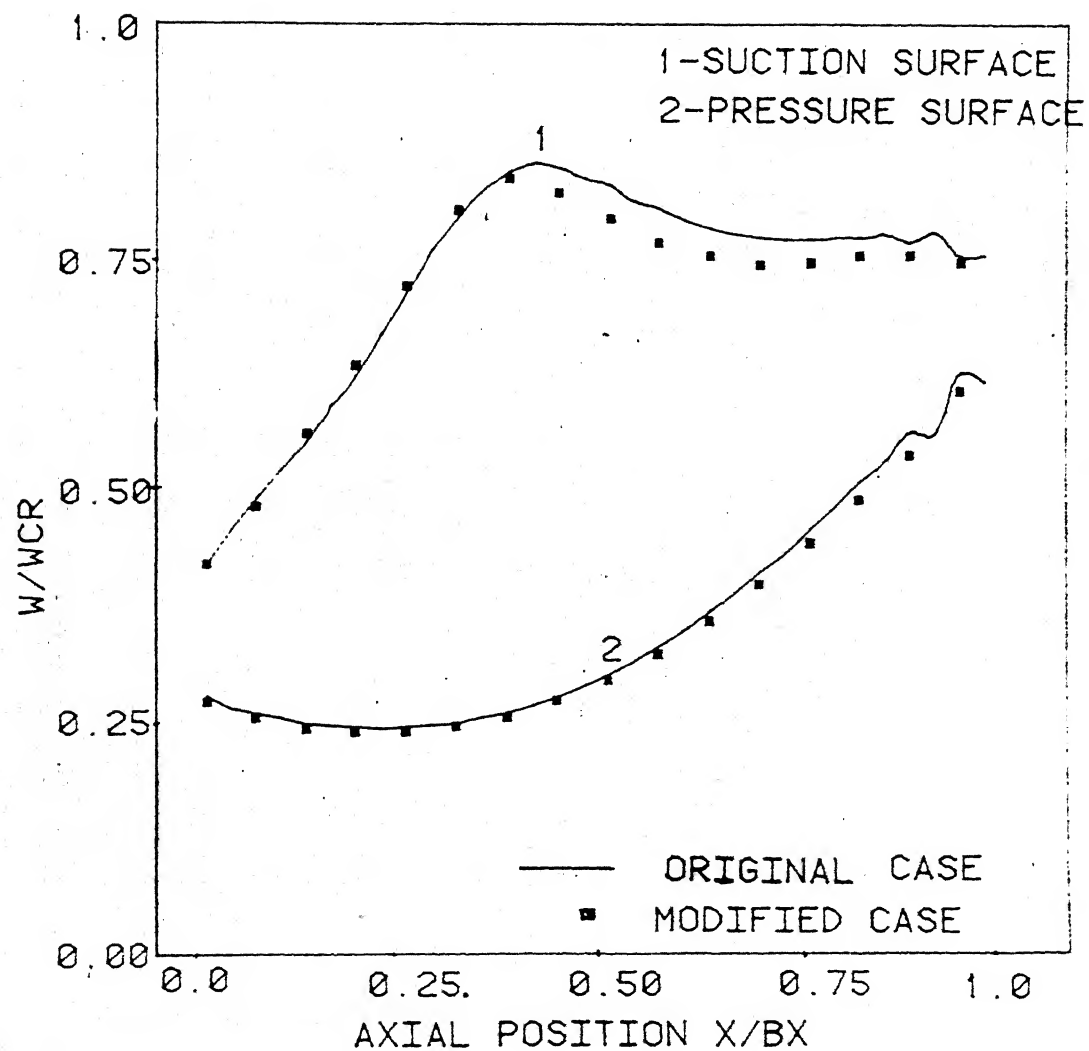


FIG 4.8 COMPARISION OF BLADE SURFACE VELOCITIES FOR ROTOR CASE

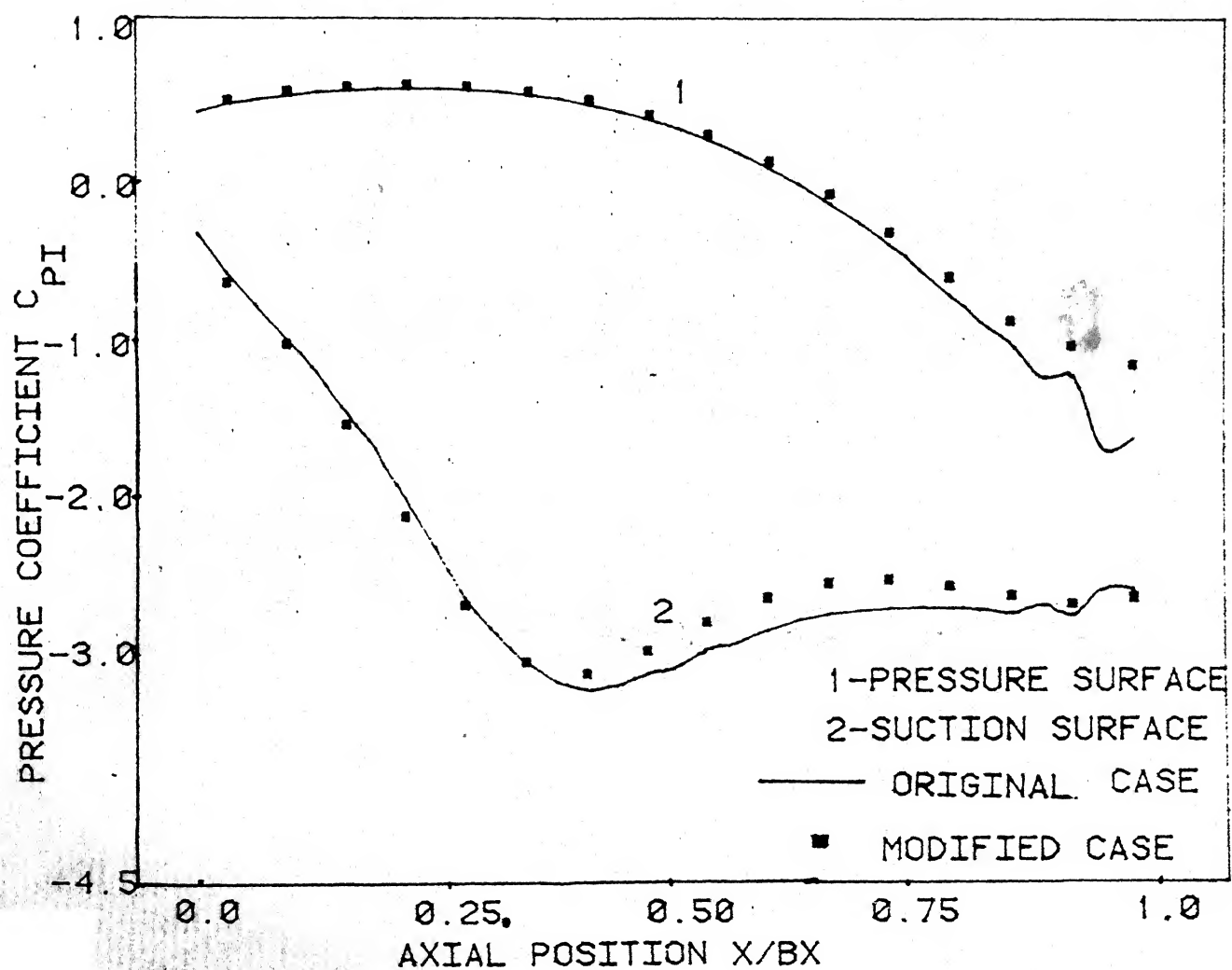


FIG 4.9 COMPARISON OF SURFACE PRESSURE COEF.  
DISTRIBUTION FOR ROTOR CASE